



PMR 5251

Assessment of Mechanical Behavior of Materials using Machine Learning Approach

Profa.Dra. Izabel Fernanda Machado and

Profa. Dra. Larissa Driemeier

Profa. Izabel Machado - machadoi@usp.br

Profa. Larissa Driemeier - driemeie@usp.br



Encyclopedia of
materials
characterization: surface
s, interfaces,
thin films / C. Richard
Brundle, Charles
A. Evans, Jr., Sham
Wilson., 1992
ISBN CL7506-9168-9

“ Though a wide range of analytical techniques is covered in this volume there are certain traits common to many of them. Most involve either electrons, photons, or ions as a probe beam striking the material to be analyzed. The beam interacts with the material in some way, and in some of the techniques the *changes* induced in the beam (energy, intensity, and angular distribution) are monitored after the interaction, and analytical information is derived from the observation of these changes. In other techniques the information used for analysis comes from electrons, photons, or ions that are ejected from the sample under the stimulation of the probe beam. In many situations several connected processes may be going on more or less simultaneously, with a particular analytical technique picking out only one aspect, e.g., the extent of absorption of incident light, or the kinetic energy distribution of ejected electrons “



Compilation of Comparative Information on the Analytical Techniques Discussed in This Volume

Article No.	Technique	Main information						Depth probed (typical)	Width probed (typical)	Trace capability (typical)	Types of solid sample (typical)	Vacuum needed ?	Commercial Instrument cost	Usage	Service available
		Elemental Chem. state	Phase	Defects	Structure	Image	Other								
2.1	Light Microscopy			•	•	•	Variable	0.2 μm	—	All	N	1	1	Y	
2.2	SEM			•	•		sub μm	10 nm	—	Cond., coated ins.	Y	2	1	Y	
2.3	STM			•	•	•	sub Å	1 Å	—	Conductors	N	2	3	Y	
2.3	SFM			•	•	•	sub Å	1 nm	—	All	N	2	2	Y	
2.4	TEM		•	•	•	•	200 nm*	5 nm	—	All; <200 nm thick	Y	3	2	Y	
3.1	EDS	•				•	1 μm	0.5 μm	500 ppm	All; Z > 5	Y	2	2	Y	
3.2	EELS	•	•			•	20 nm*	1 nm	Few %	All; <30 nm thick	Y	2	3	N	
3.3	Cathodo-luminescence	•		•		•	10 nm–μm	1 μm	ppm	All; semicond. usually	Y	1	3	N	
3.4	STEM		•	•	•	•	100 nm*	1 nm	—	All; <200 nm thick	Y	3	3	N	
3.5	EPMA	•				•	1 μm	0.5 μm	100 ppm	All; flat best	Y	3	2	Y	
4.1	XRD		•	•	•		10 μm	mm	3%	Crystalline	N	2	1	Y	
4.2	EXAFS	•			•		Bulk*	mm	Few %	All	Y/N	—	3	N	
4.3	SEXAFS	•			•		1 nm	mm	Few %	Surface and adsorbate	Y	—	3	N	
4.3	NEXAFS	•	•		•		1 nm	mm	Few %	Surface and adsorbate	Y	—	3	N	
4.4	XPD	•	•		•		3 nm	150 μm	1%	Single crystal	Y	3	3	N	
4.5	LEED			•	•		1 nm	0.1 mm	—	Single crystal	Y	—	2	N	
4.6	RHEED			•	•		1 nm	0.02 mm	—	Single crystal	Y	—	2	N	
5.1	XPS	•	•				3 nm	150 μm	1%	All	Y	3	1	Y	
5.2	UPS	•			•		1 nm	mm	—	All	Y	—	3	N	
5.3	AES	•	•			•	2 nm	100 nm	0.1%	All, inorganic usually	Y	3	1	Y	

Materials Characterization

Encyclopedia of materials characterization: surface s, interfaces, thinfilms/C. Richard Brundle, Charles A. Evans, Jr., Sham Wilson., 1992 ISBN CL7506-9168-9



Materials Characterization

Encyclopedia of
materials
characterization: surface
s, interfaces,
thinfilms/C. Richard
Brundle, Charles
A. Evans, Jr., Sham
Wilson., 1992
ISBN CL7506-9168-9

Compilation of Comparative Information on the Analytical Techniques Discussed in This Volume

Article No.	Technique	Main information						Depth probed (typical)	Width probed (typical)	Trace capability (typical)	Types of solid sample (typical)	Vacuum needed ?	Commercial Instrument cost	Usage	Service available
		Elemental Chem. state	Phase	Defects	Structure	Image	Other								
5.4	REELS	• •				•	2 nm	100 nm	—	All	Y	—	3	N	
6.1	XRF	•					10 μm	mm	0.1%	All	N	2	1	Y	
6.2	TXRF	•					3 nm	cm	ppb–ppm	Trace heavy metals	Y	3	3	Y	
6.3	PIXE	•					Few μm	100 μm	10 ppm	All	Y	3	3	Y	
7.1	Photo-luminescence	•		•		• •	Few μm	Few μm	ppb	All, semicond. usually	N	1	2	N	
7.2	Modulation Spectroscopy	•		•		• •	1 μm	100 μm	ppm	All, semicond. usually	N	2	3	N	
7.3	VASE						1 μm	cm	—	Flat thin films	N	2	3	Y	
8.1	FTIR	•		•		•	Few μm	20 μm	Variable	All	N	2	1	Y	
8.2	Raman Scattering	•		•		•	Few μm	1 μm	Variable	All	N	2	2	Y	
8.3	HREELS	•			•		2 nm	mm	1%	All; flat cond. best	Y	3	3	N	
8.4	NMR	• •			•		Bulk	—	—	All; not all elements	N	3	3	N	
9.1	RBS	•		• •			To 2 μm	mm	0.01–10%	All	Y/N	3	2	Y	
9.2	ERS					•	1 μm	mm	0.01%	H containing	Y	—	3	N	
9.3	MEIS	•		• •			1 nm	mm	0.1%–10%	All; usually single crystal	Y	3	3	N	
9.4	ISS	•					3 Å	150 μm	50 ppm–1%	All	Y	—	3	Y	
10.1	Dynamic SIMS	•				•	2 nm	1 μm	ppb–ppm	All, mostly semicond.	Y	3	1	Y	
10.2	Static SIMS	• •				•	3 Å	100 μm	Few %	All, mostly polymer	Y	3	2	Y	
10.3	SALI	• •					3 Å	100 nm	ppb–ppm	All, mostly inorg.	Y	3	3	N	



Compilation of Comparative Information on the Analytical Techniques Discussed in This Volume

Article No.	Technique	Main information						Depth probed (typical)	Width probed (typical)	Trace capability (typical)	Types of solid sample (typical)	Vacuum needed?	Commercial Instrument cost	Usage	Service available
		Elemental Chem. state	Phase	Defects	Structure	Image	Other								
10.4	SNMS	•						1.5 nm	cm	50 ppm	Flat conductors	Y	2	2	Y
10.5	LIMS	• •						100 nm	2 μm	1–100 ppm	All	Y	3	2	Y
10.6	SSMS	•						3 μm	cm	0.05 ppm	Sample forms electrode	Y	—	2	Y
10.7	GDMS	•						100 nm	cm	ppt–ppb	Sample forms electrode	Y	3	2	Y
10.8	ICPMS	•						5 μm	mm	ppt	All	Y	2	1	Y
10.9	ICPOES	•						5 μm	mm	ppb	All	Y	1	1	Y
11.1	Neutron Diffraction		•	•				Bulk	—	—	Crystalline	N	—	3	N
11.2	Neutron Reflectivity						•	Up to mm	—	—	Flat polymer films	N	—	3	N
11.3	NAA	•						Bulk	—	ppt–ppm	Trace metals	N	2	3	Y
11.4	NRA	•						10–100 nm	10 μm	10–100 ppm	All; Z < 21	Y	—	3	Y
12.2	Optical Scatterometry						•	—	mm	—	Flat smooth films	N	1	3	Y
12.3	MOKE						• •	30 nm	0.5 μm	—	Magnetic films	N	1	2	N
12.4	Adsorption						•	Outer atoms	—	—	Large surface area	Y	—	2	N

Notes: This table should be used as a “quick reference” guide only.

* Measured in transmission.

Commercial Instrument cost: These are typical costs; large ranges depending on sophistication and accessories: 1 means < \$50k; 2 means \$50–300k; 3 means >\$300k. “—” means no complete commercial instrument.

Usage: Numbers refer to usage for analysis of solid materials. 1 means Extensive; 2 means medium; 3 means not common.

Trace capability: Guide only. Often very material/conditions dependent. “—” means not used for trace components.

Materials Characterization

Encyclopedia of materials characterization: surfaces, interfaces, thinfilms/C. Richard Brundle, Charles A. Evans, Jr., Sham Wilson., 1992 ISBN CL7506-9168-9

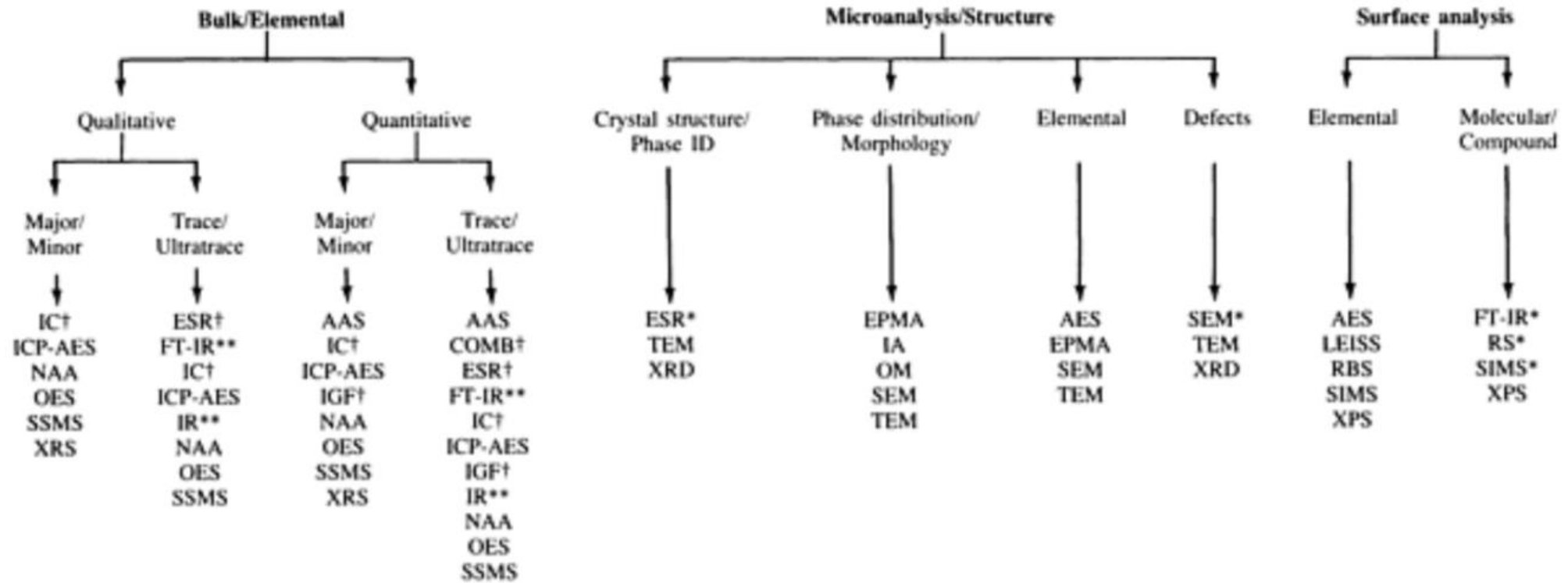


Fig. 1 Flow chart of inorganic solids: metals, alloys, semiconductors. Acronyms are defined in Table 10.

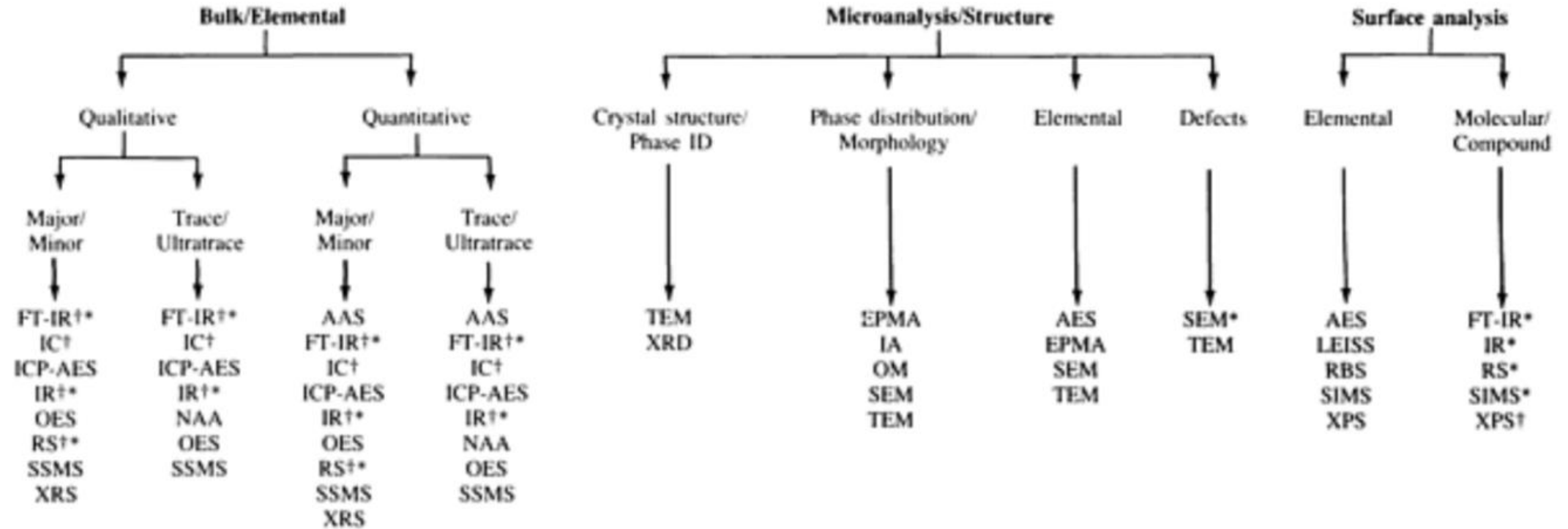


Fig. 2 Flow chart of inorganic solids: glasses, ceramics. Acronyms are defined in Table 10.

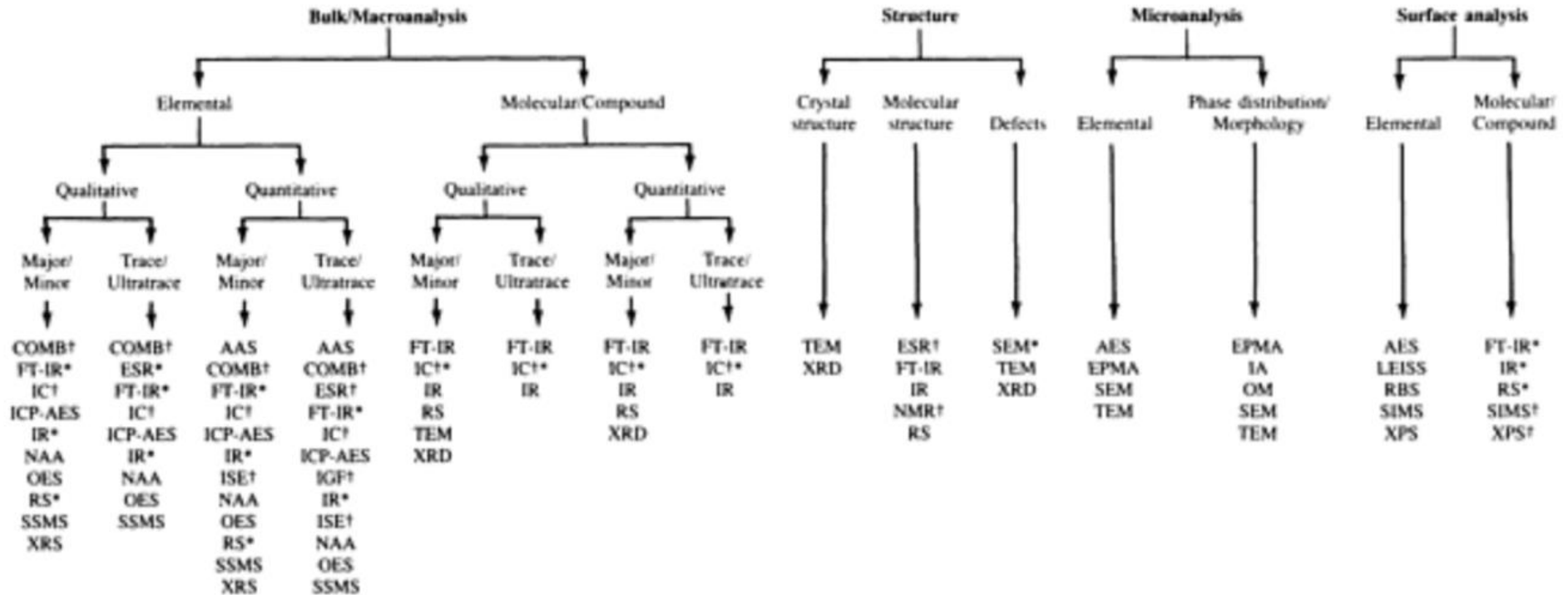


Fig. 3 Flow chart of inorganic solids: minerals, ores, slags, pigments, inorganic compounds, effluents, chemical reagents, composites, catalysts. Acronyms are defined in Table 10.



ASM Handbook vol.
10 – Materials
Characterization

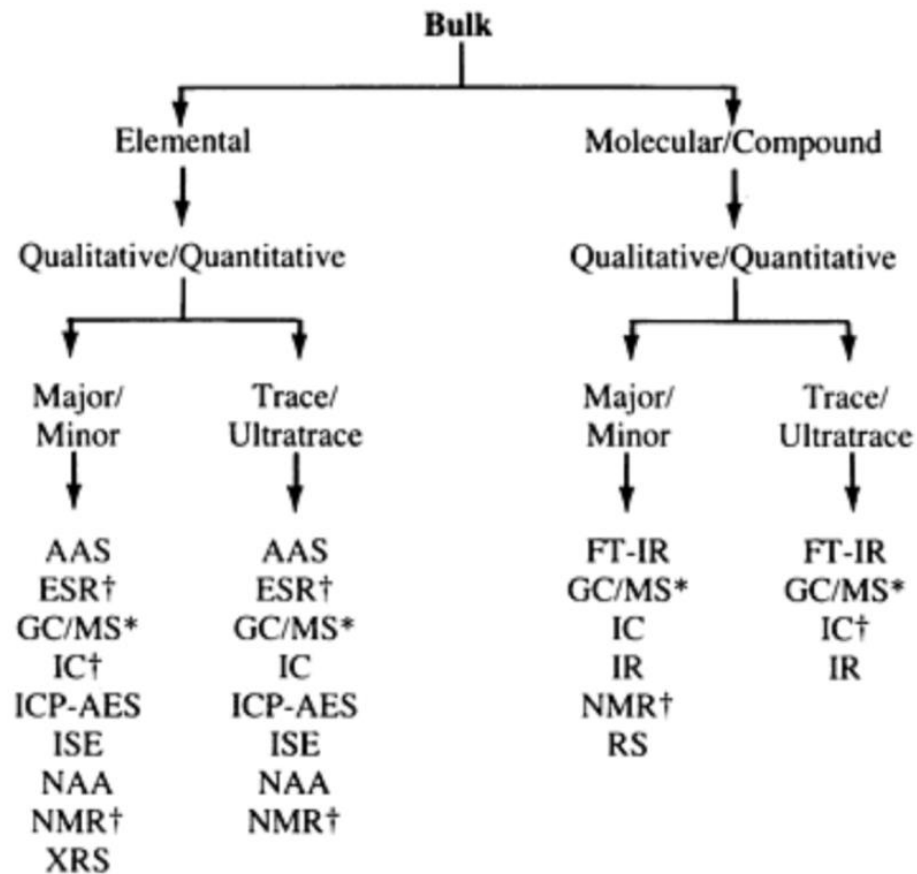


Fig. 4 Flow chart of inorganic liquids and solutions: water, effluents, leachates, acids, bases, chemical reagents. Acronyms are defined in Table 10.

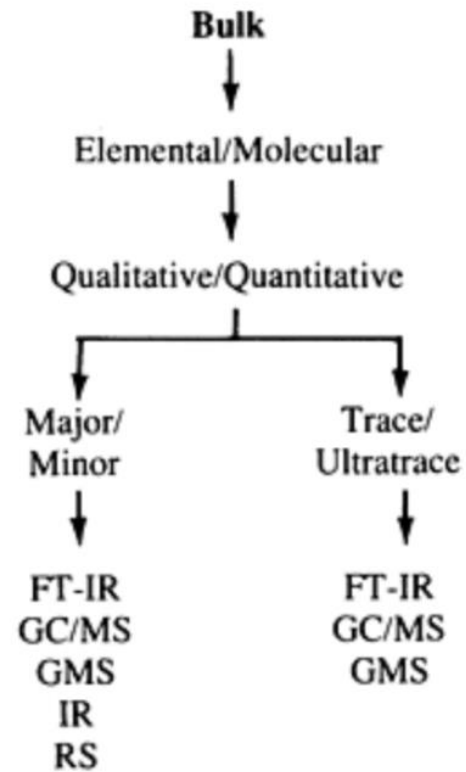


Fig. 5 Flow chart of inorganic gases: air, effluents, process gases. Acronyms are defined in Table 10.

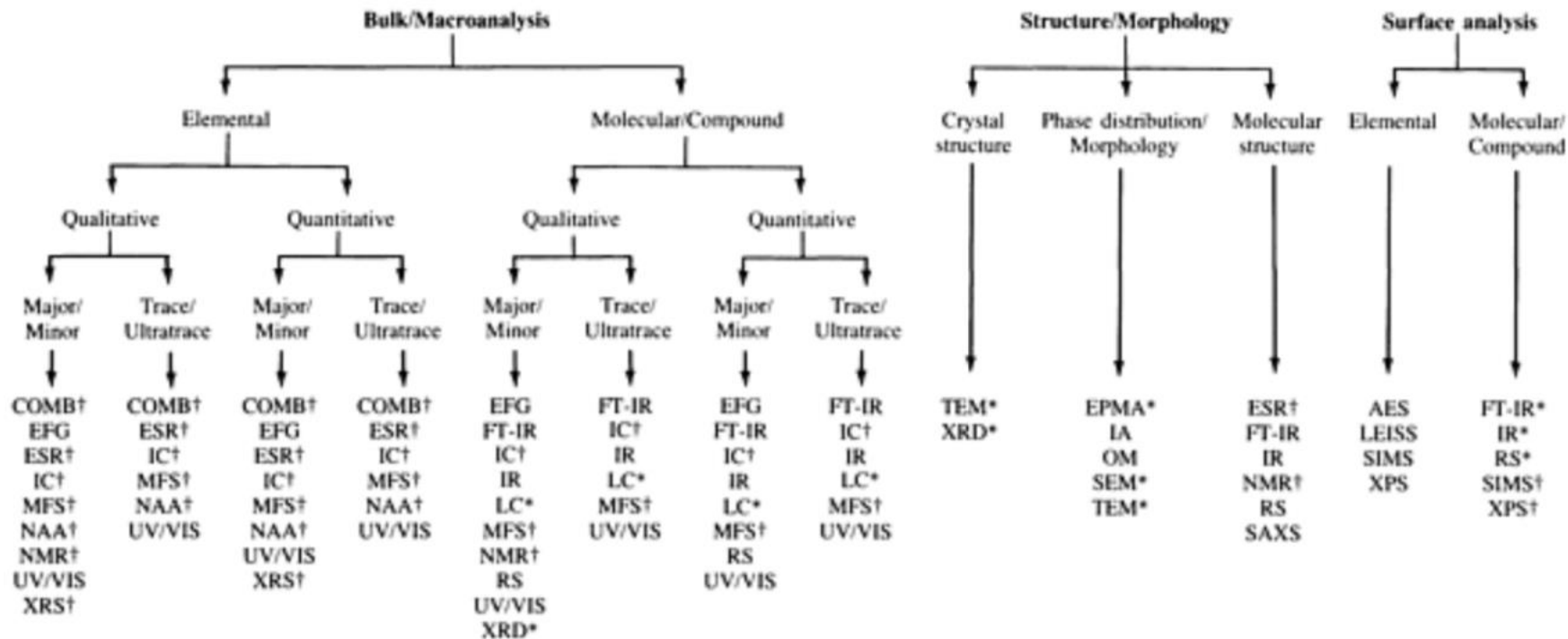


Fig. 6 Flow chart of organic solids: polymers, plastics, epoxies, long-chain hydrocarbons, esters, foams, resins, detergents, dyes, organic composites, coal and coal derivatives, wood products, chemical reagents, organometallics. Acronyms are defined in Table 10.



ASM Handbook vol.
10 – Materials
Characterization

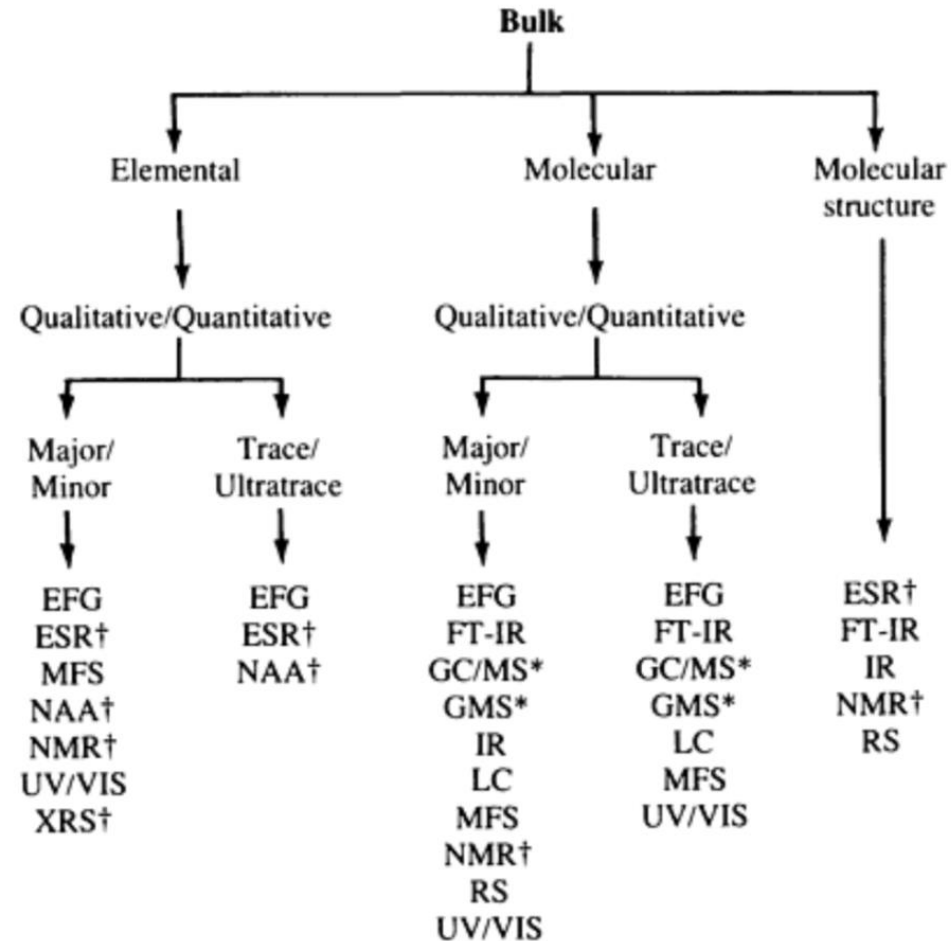


Fig. 7 Flow chart of organic liquids and solutions: hydrocarbons, petroleum and petroleum derivatives, solvents, reagents. Acronyms are defined in Table 10.



General analyses



FT-IR
GC/MS
GMS
IR
LC
RS

Fig. 8 Flow chart of organic gases: natural gas, effluents, pyrolysis products, process gas. Acronyms are defined in Table 10.



Light Microscopy

The light microscope uses the visible or near visible portion of the electromagnetic spectrum; light microscopy is the interpretive use of the light microscope

the first polished metal and metal-alloy specimens were prepared and viewed with the intention of correlating their structures with their properties

Range of samples characterized	Almost unlimited for solids and liquid crystals
Destructive	Usually nondestructive; sample preparation may involve material removal
Quantification	Via calibrated eyepiece micrometers and image analysis
Detection limits	To sub-ng
Resolving power	0.2 μm with white light
Imaging capabilities	Yes
Main use	Direct visual observation; preliminary observation for final characterization, or preparative for other instrumentation
Instrument cost	\$2,500–\$50,000 or more
Size	Pocket to large table

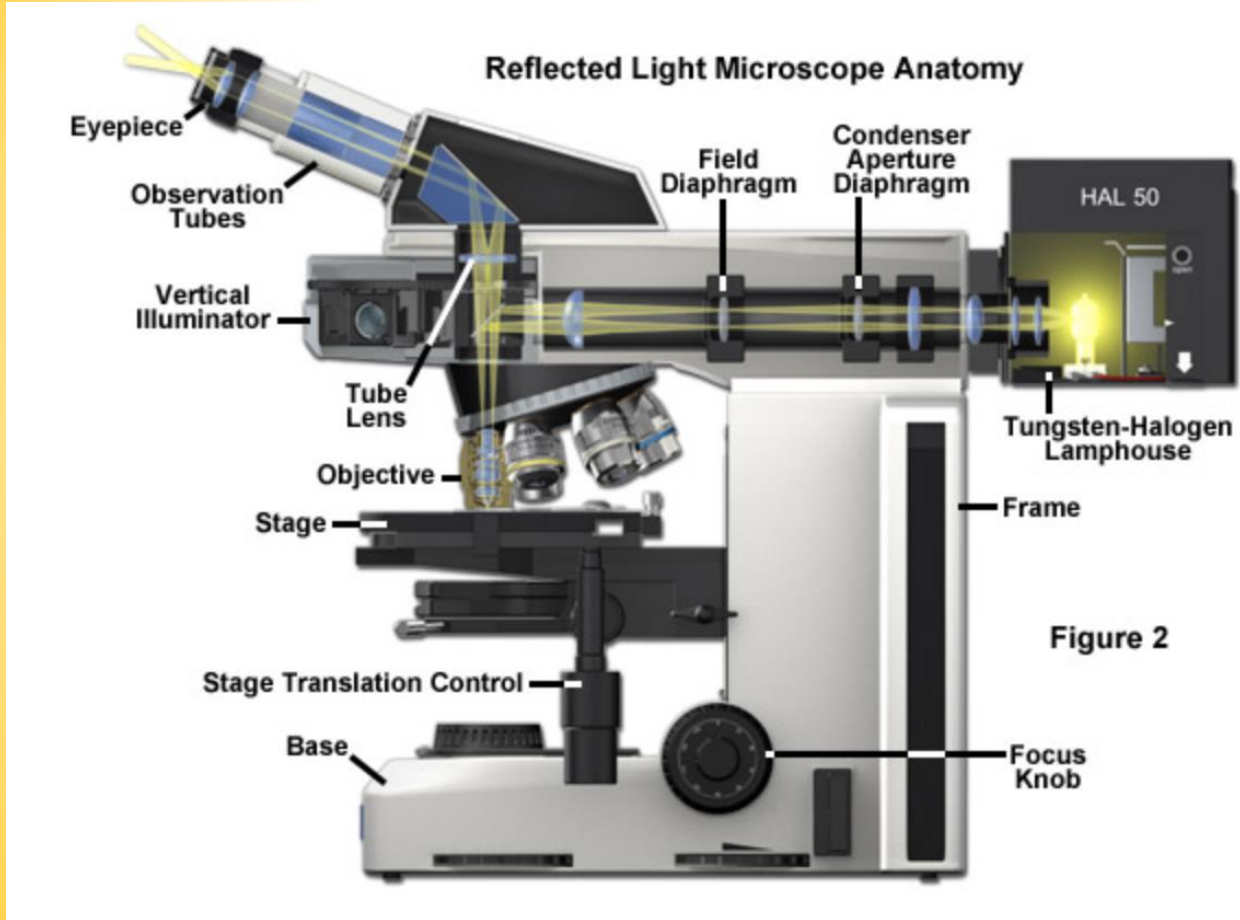
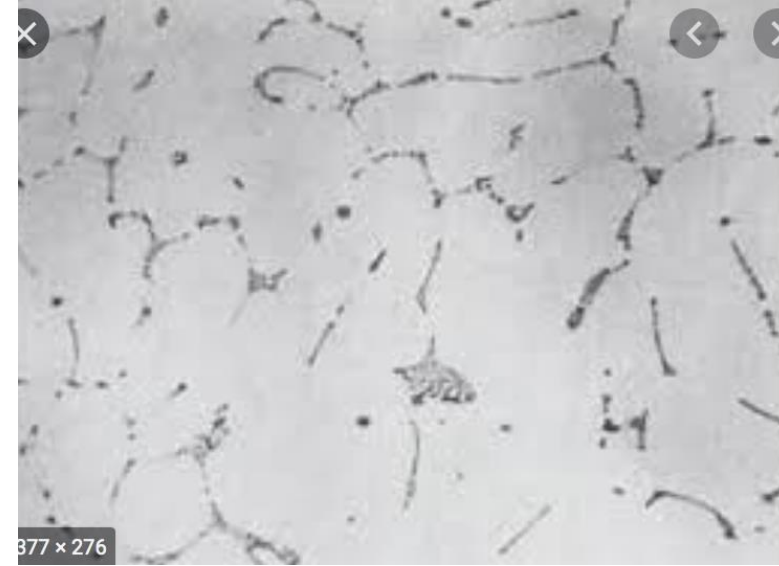
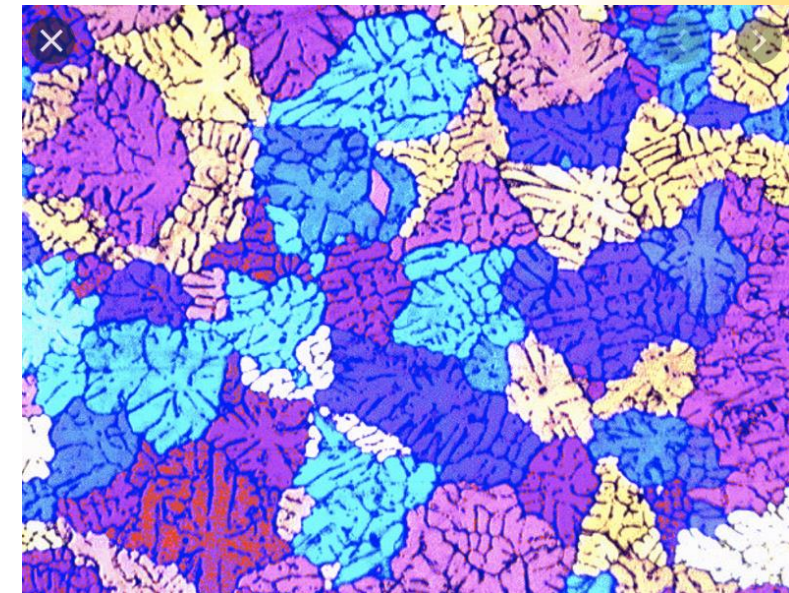


Figure 2



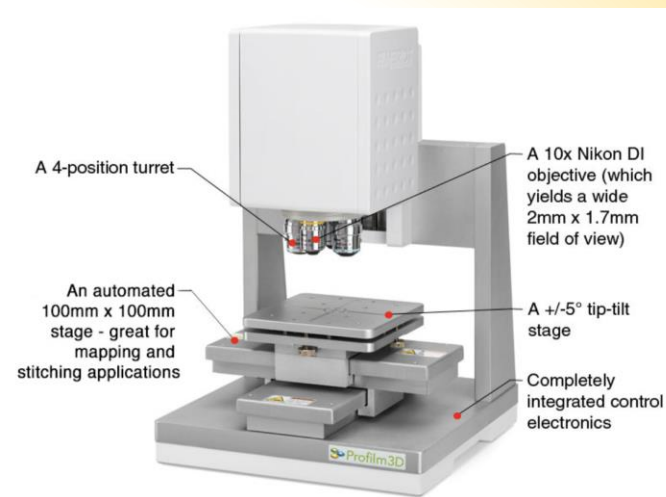
Al alloys



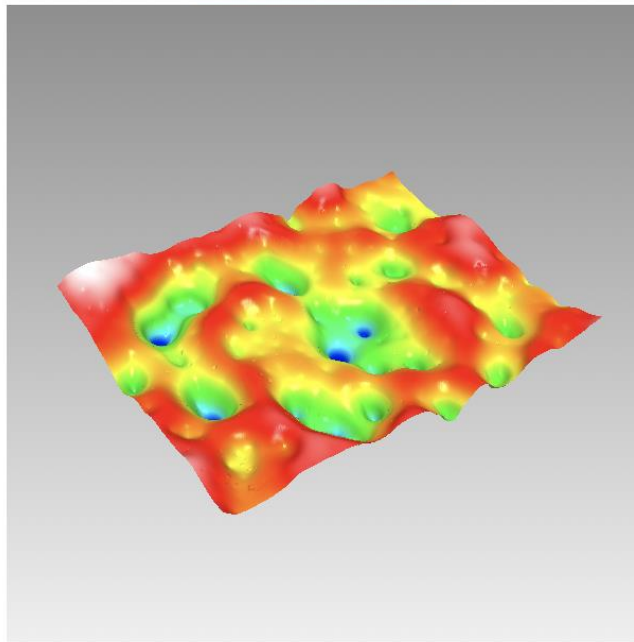
<http://zeiss-campus.magnet.fsu.edu/articles/basics/reflected.html>



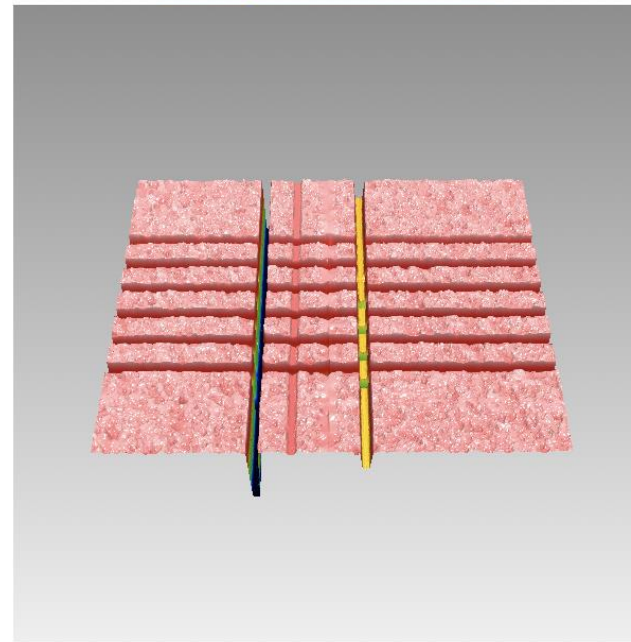
Profilometer



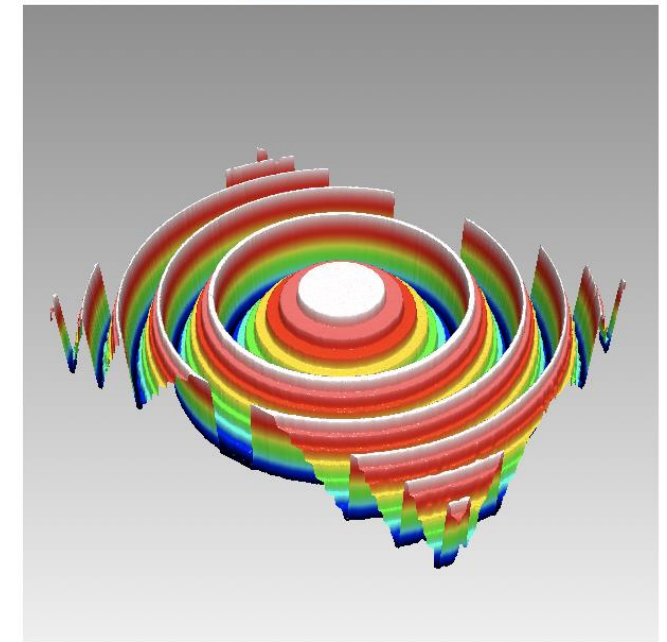
Ceramic Surface



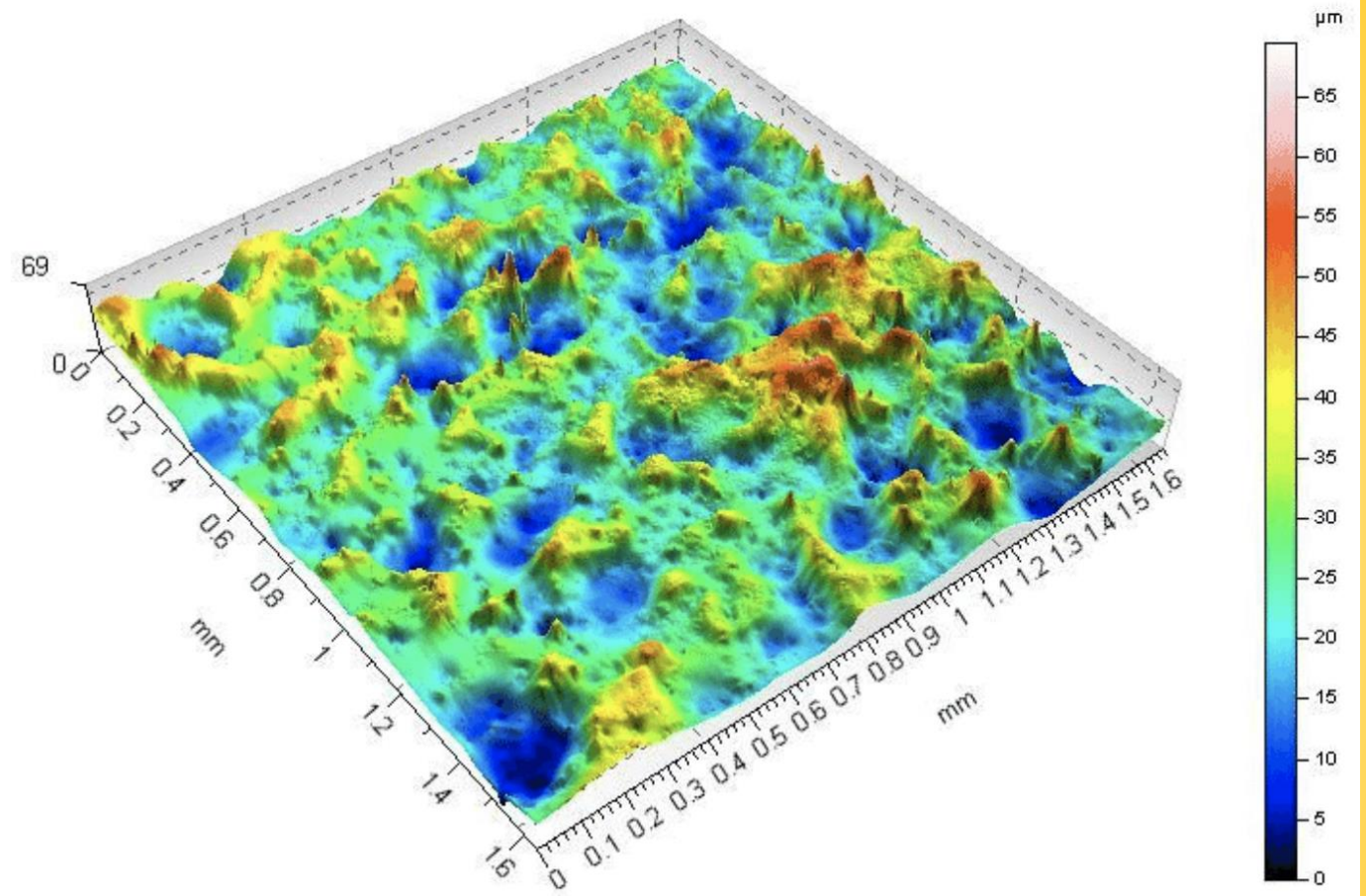
Dicing-Saw Test Cuts



Fresnel Lens

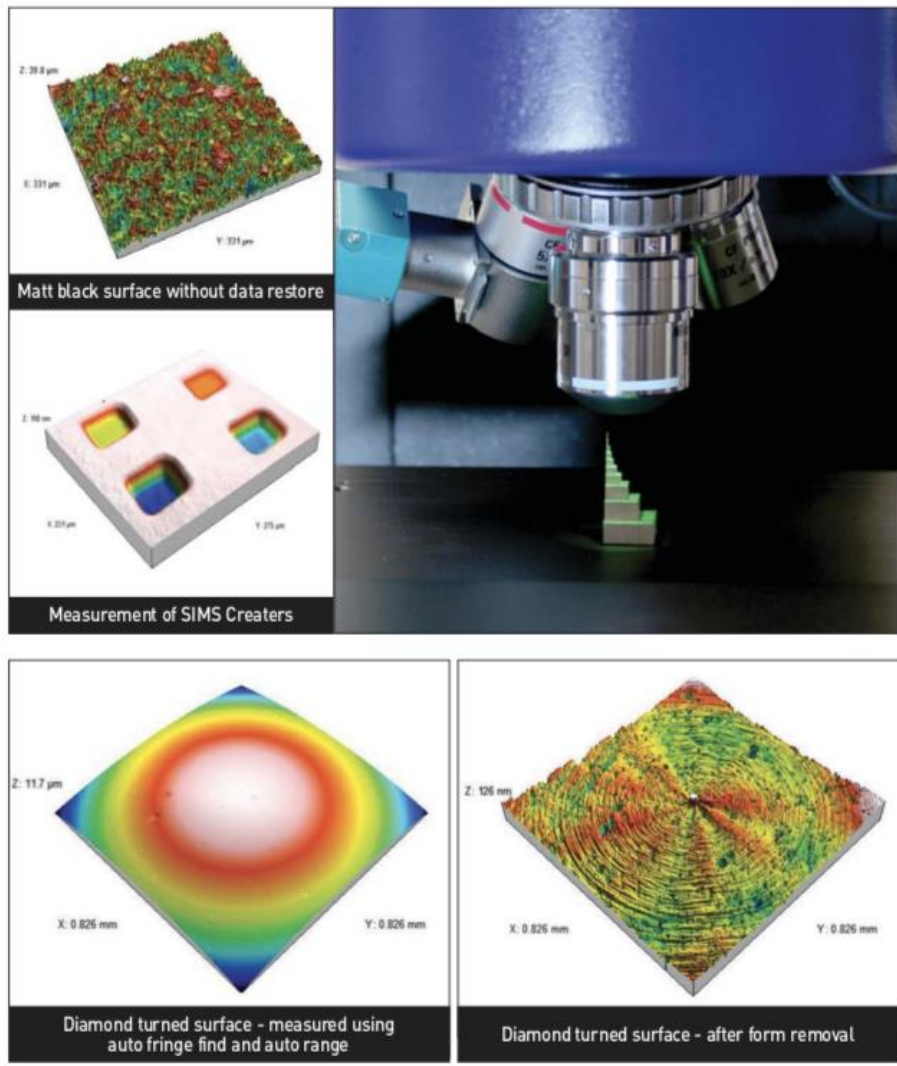


https://www.filmetrics.com/profilometers/profilm3d?gclid=EAlaIQobChMIzNvtpOT_6wIVS4CRCh2Lhg99EAAAYASAAEgKqXPD_BwE



View of 3D on machined surface made by Talysurf CCI Lite-Taylor Hobson scanning profilometer type

https://www.researchgate.net/figure/ew-of-3D-on-machined-surface-made-by-Talysurf-CCI-Lite-Taylor-Hobson-scanning_fig1_313649778



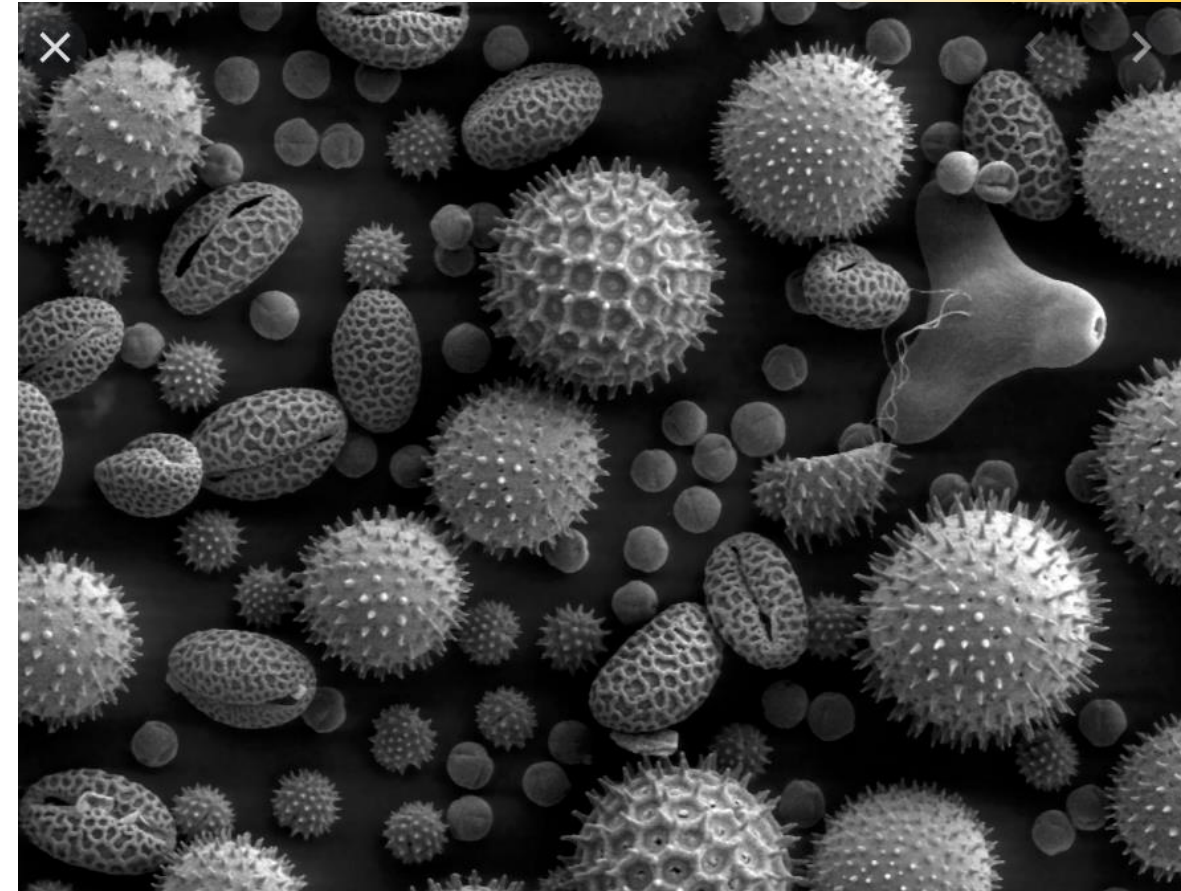
Talysurf CCI Lite System Specifications	
Measurement technique	Coherence Correlation Interferometry
Vertical range [Z]	2.2 mm as standard (>10 mm with Z-stitching)
Vertical resolution [max]	0.01 nm [0.1 Å]
Noise floor [Z]	<0.08 nm [0.8 Å] ¹
Repeatability of surface RMS [Z]	<0.02 nm [0.2 Å] ²
Max. Measurement area [X, Y]	6.6 mm (>75 mm with X, Y stitching)
Number of measurement points	1024 x 1024 standard
Optical resolution [X, Y]	0.4 - 0.6 μm (surface dependent)
Step height repeatability	<0.1%
Surface reflectivity	0.3% - 100%
Measurement time	5-40 seconds (typical)

¹ As demonstrated by multiple measurements on a levelled fused silica optical flat
² As demonstrated by 1 sigma Std Dev of 20 Sq (RMS) measurements on SiC flat



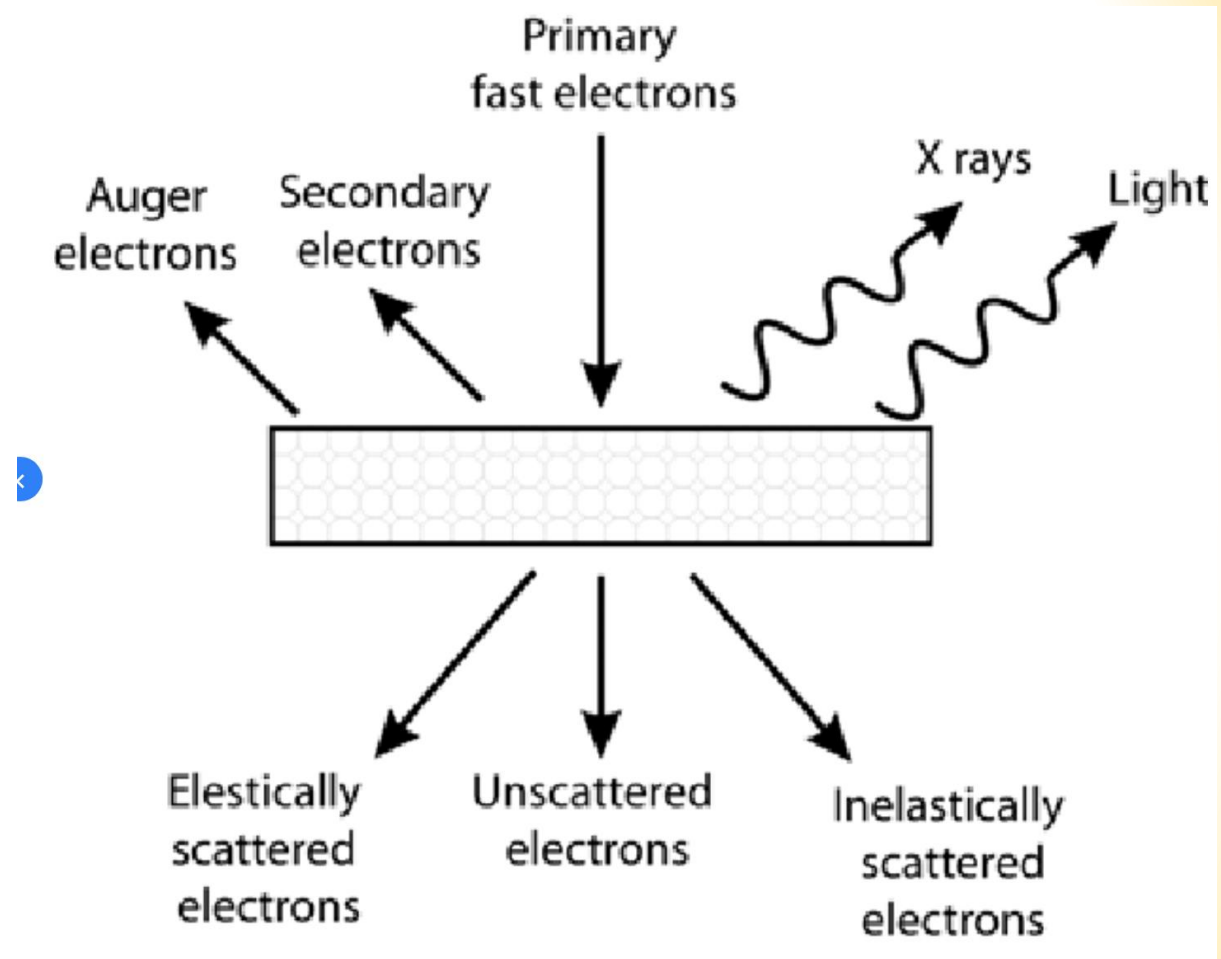
The Scanning Electron Microscope (SEM) is often the first analytical instrument used when a "quick look" at a material is required and the light microscope no longer provides adequate resolution. In the SEM an electron beam is focused into a fine probe and subsequently raster scanned over a small rectangular area. As the beam interacts with the sample it creates various signals (secondary electrons, internal currents, photon emission, etc.), all of which can be appropriately detected. These signals are highly localized to the area directly under the beam.

Main use	High magnification imaging and composition (elemental) mapping
Destructive	No, some electron beam damage
Magnification range	10×–300,000×; 5000×–100,000× is the typical operating range
Beam energy range	500 eV–50 keV; typically, 20–30 keV
Sample requirements	Minimal, occasionally must be coated with a conducting film; must be vacuum compatible
Sample size	Less than 0.1mm, up to 10 cm or more
Lateral resolution	1–50 nm in secondary electron mode
Depth sampled	Varies from a few nm to a few μm, depending upon the accelerating voltage and the mode of analysis
Bonding information	No
Depth profiling capabilities	Only indirect
Instrument cost	\$100,000–\$300,000 is typical
Size	Electronics console 3 ft. × 5 ft.; electron beam column 3 ft. × 3 ft.

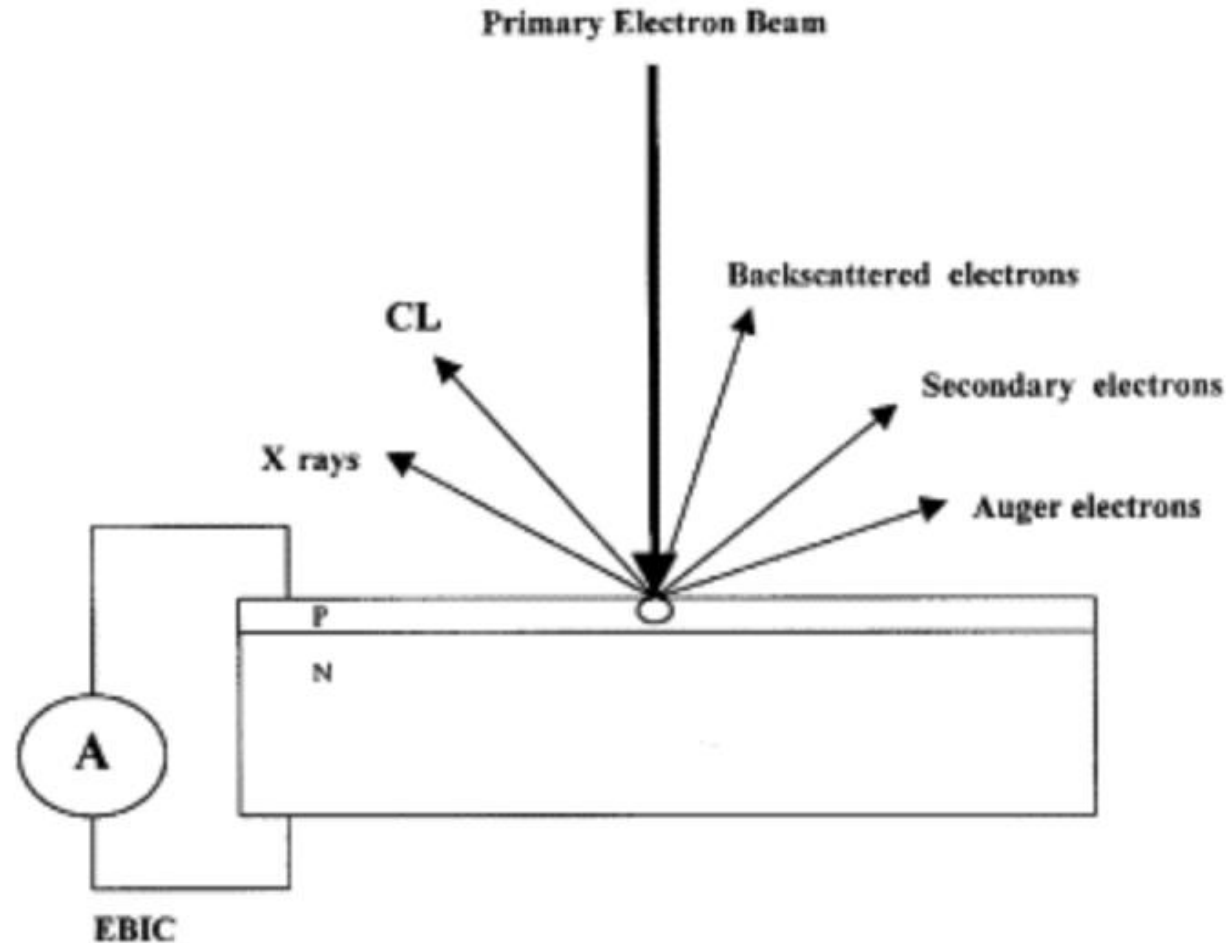




Simplified electron beam-sample interaction: secondary electrons, auger electrons, light photons and X-rays are emitted from the sample when this is struck by fast incoming electrons. Transmitted electrons can remain unscattered, or be elastically or inelastically scattered.

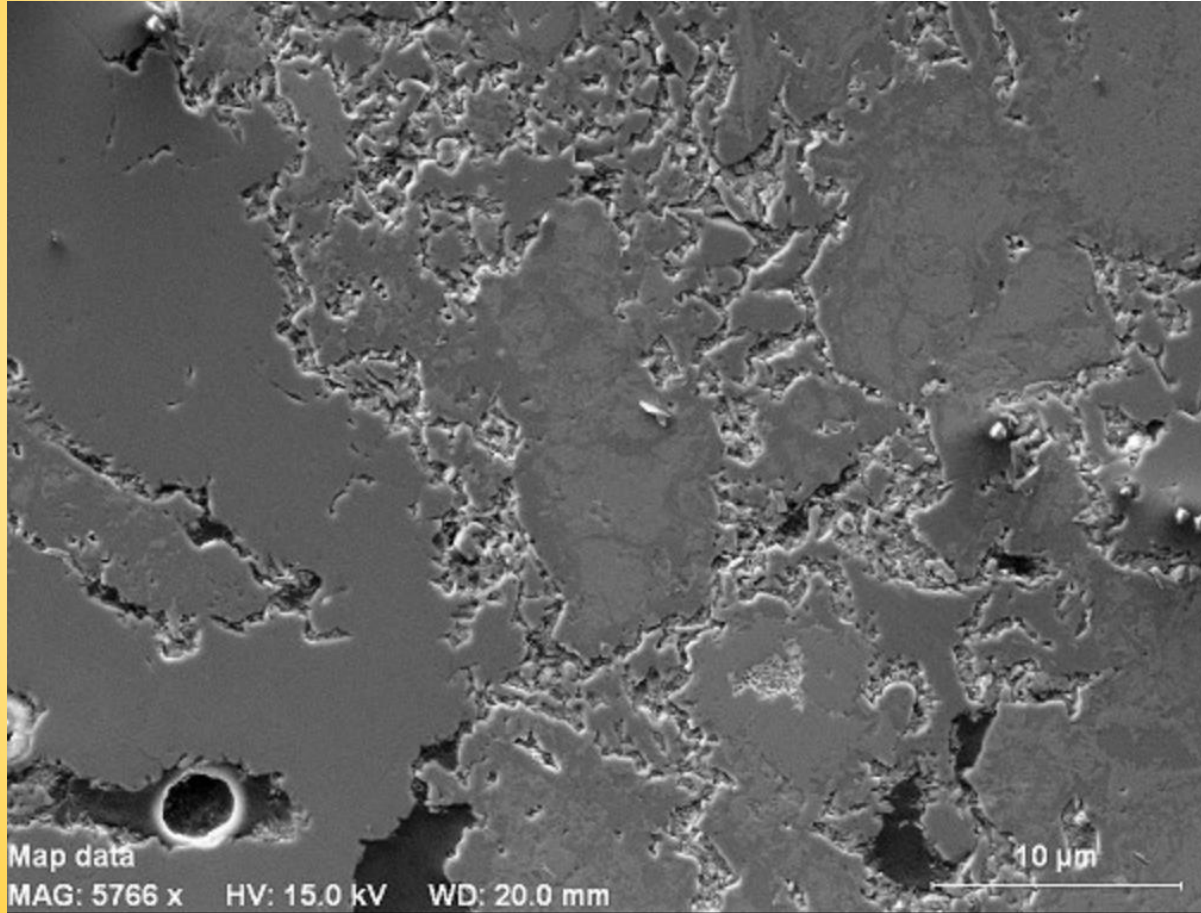
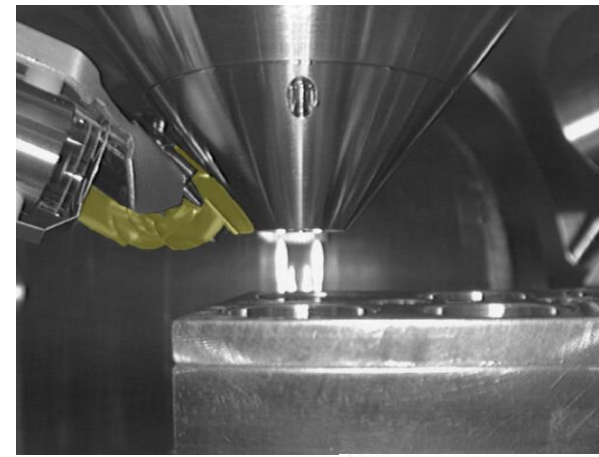


https://www.researchgate.net/figure/Simplified-electron-beam-sample-interaction-secondary-electrons-auger-electrons-light_fig5_289520567





Secondary electrons

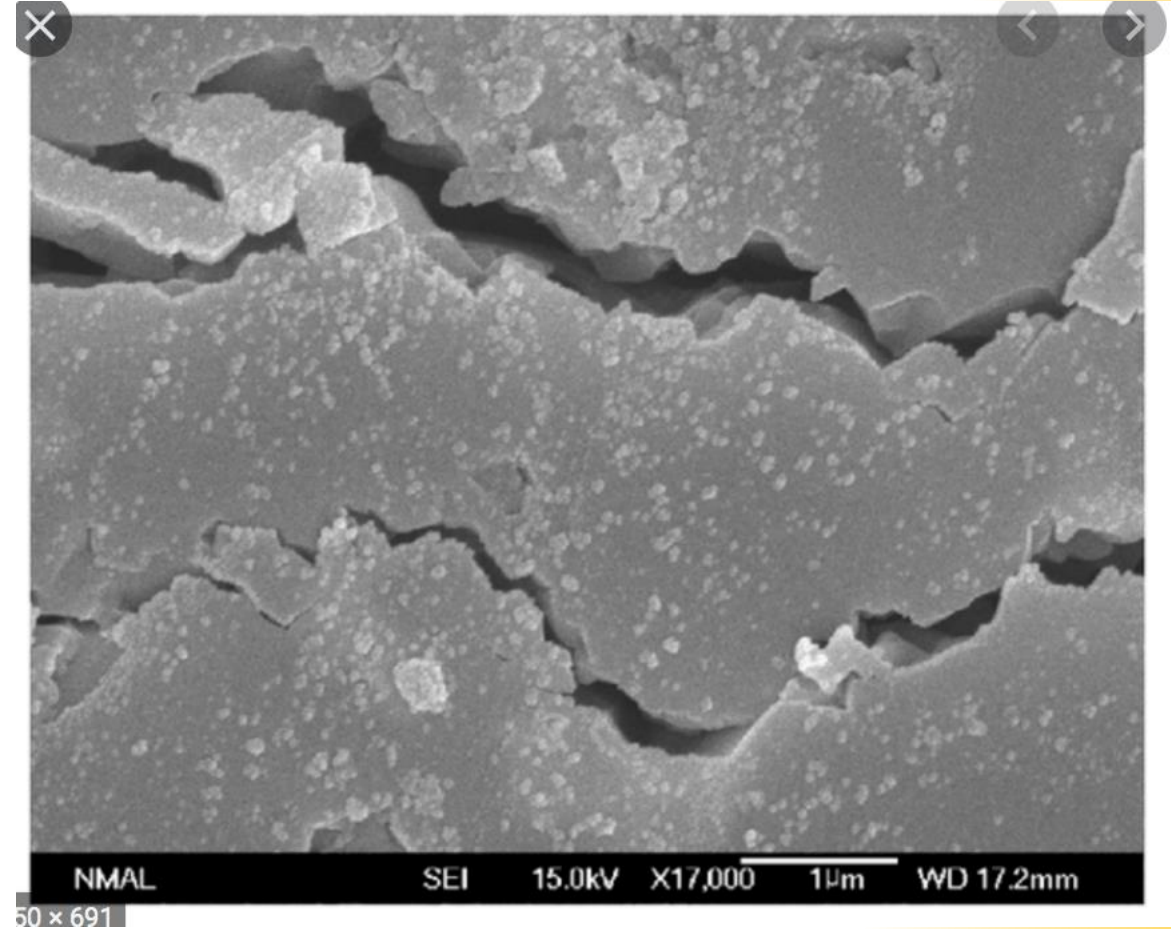
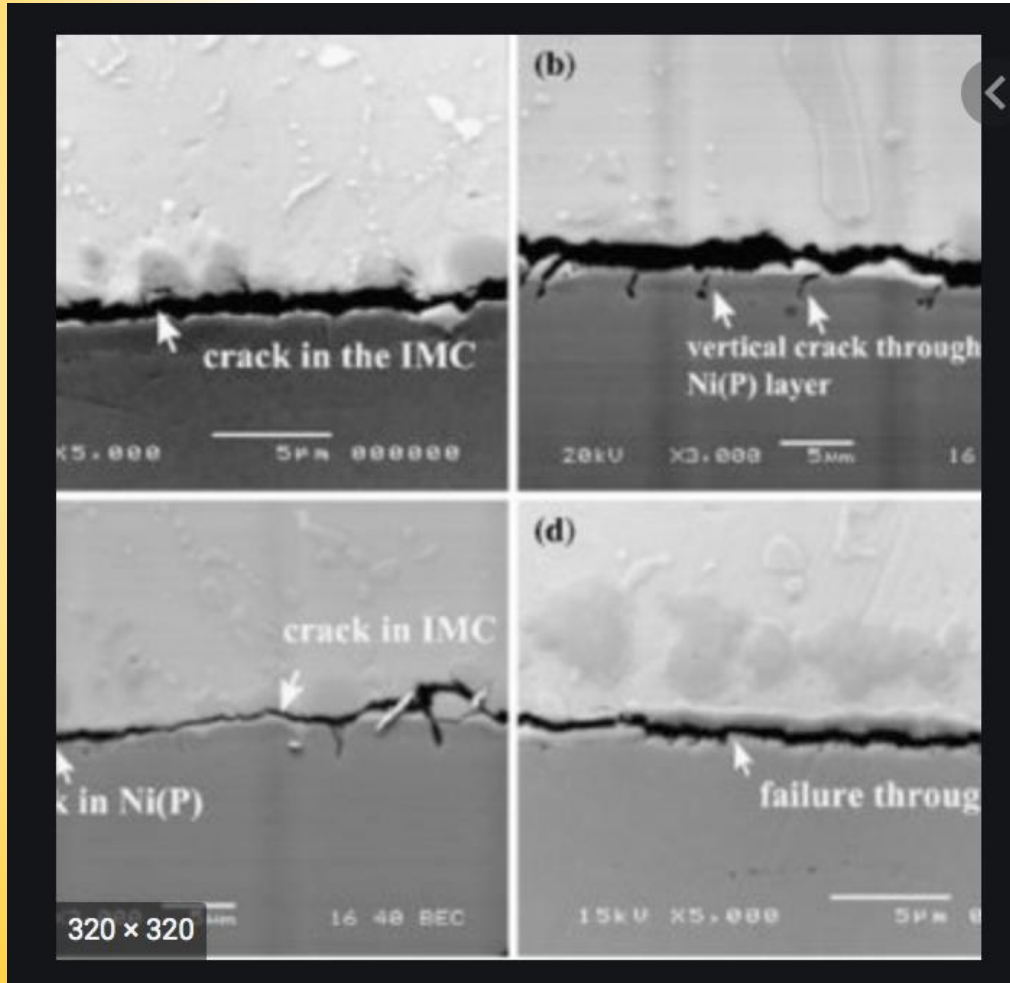


This is an image of an aluminum copper alloy formed using backscattered electron imaging. The light area is mostly copper and the dark area is mostly aluminum.

<http://minerva.union.edu/hollochk/sem/se.html>



Surface Analysis





Energy dispersive spectrometers (**EDS**) sort the X-rays based on their energy; while wavelength dispersive spectrometers (**WDS**) sort the X-rays based on their wavelengths.

Table 3110. Comparison between EDS and WDS techniques.

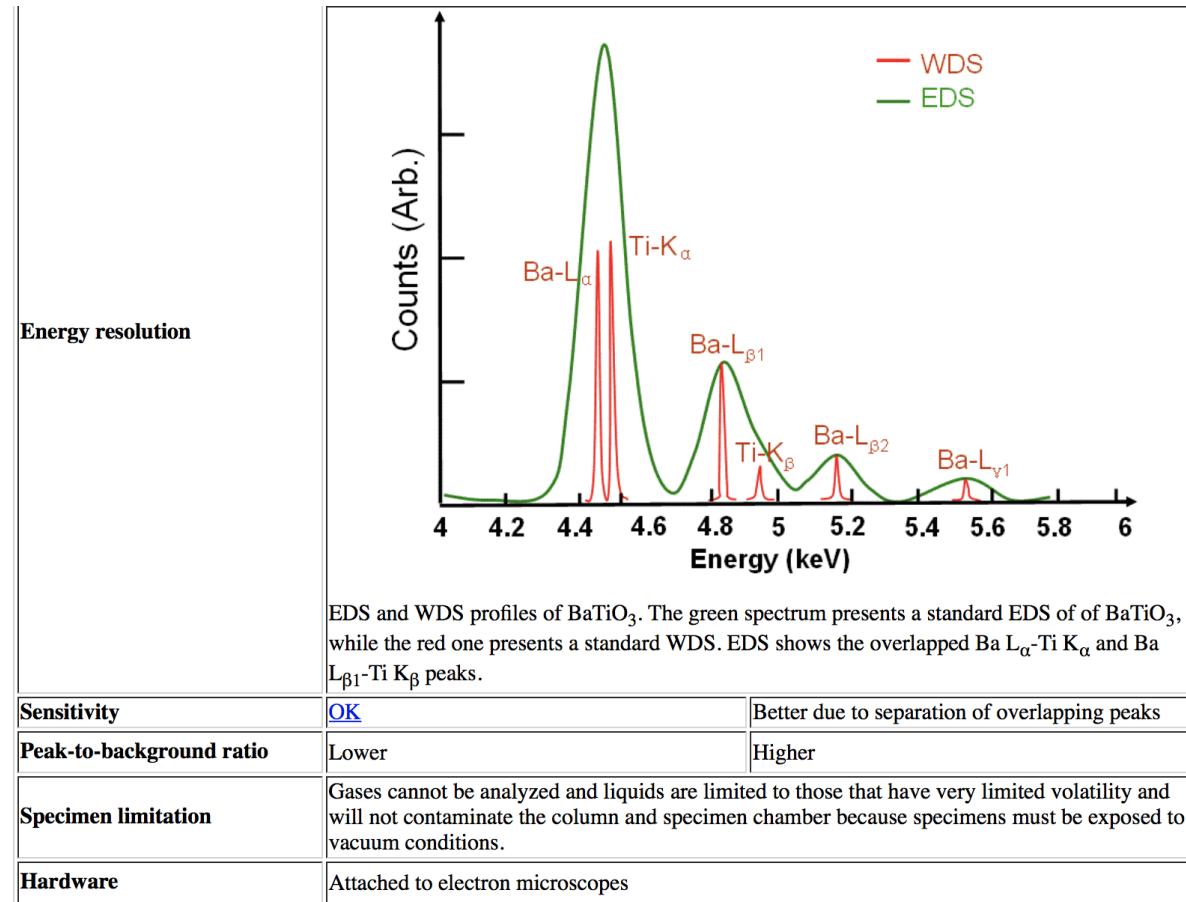
	EDS	WDS
Full name	Energy dispersive X-ray spectroscopy	Wavelength dispersive X-ray spectroscopy
Principle	Measures the energy of X-ray photon	Determine the wavelength of X-ray
Spectrum range	Measures across a broad range of energies in the spectrum	Measures specific regions within the spectrum
Efficiency	More efficient for an unknown specimen	More efficient for the concentration of specific, known element
Speed	Quicker for large energy ranges	Slower for large energy ranges
Throughput of X-rays	Lower	Higher
Spatial resolution	The same	
	Lower: ~ 125 eV	Higher: ~5-10 eV

<https://www.globalsino.com/EM/page3110.html>



Energy dispersive spectrometers (**EDS**) sort the X-rays based on their energy; while wavelength dispersive spectrometers (**WDS**) sort the X-rays based on their wavelengths.

<https://www.globalsino.com/EM/page3110.html>





Field Emission Electron Microscopy FIB e EBSD

Electron Source & Operating HT: Field emission gun 1kV~30kV

Electron beam resolution

- High-vacuum
- 1.2 nm at 30 kV (SE)
- 2.5 nm at 30 kV (BSE)*
- 2.9 nm at 1 kV (SE)
- Low-vacuum
- 1.5 nm at 30 kV (SE)
- 2.5 nm at 30 kV (BSE)
- 2.9 nm at 3 kV (SE)

•Extended low-vacuum mode (ESEM)

1.5 nm at 30 kV (SE)

Focus Ion Beam resolution:

•7 nm at 30 kV at beam coincident point (5 nm achievable at optimal working distance)

Electron optics

- High-resolution field emission – SEM column optimized for high-brightness/ high-current
- 60 degree objective lens geometry with through-the-lens differential pumping and heated objective apertures

Ion optics

- High-current ion column with Ga liquid-metal ion source
- Acceleration voltage: 2 – 30 kV
- Probe current: 1 pA – 65 nA in 15 steps
- 15-position aperture strip
- Magnification 40 x – 1280 kx in "quad" mode at 10 kV

Detectors and Attachments:

- Everhardt-Thornley SED
- Low-vacuum SED (used in low vacuum)
- Gaseous SED (GSED) (used in ESEM mode)
- Solid-State BSED
- Gaseous analytical BSED (GAD) (used for low-vacuum analytical applications)
- EDS: Oxford silicon drift detector (50 mm²) and INCA software
- HKL EBSD (Electron Backscatter Diffraction) systems

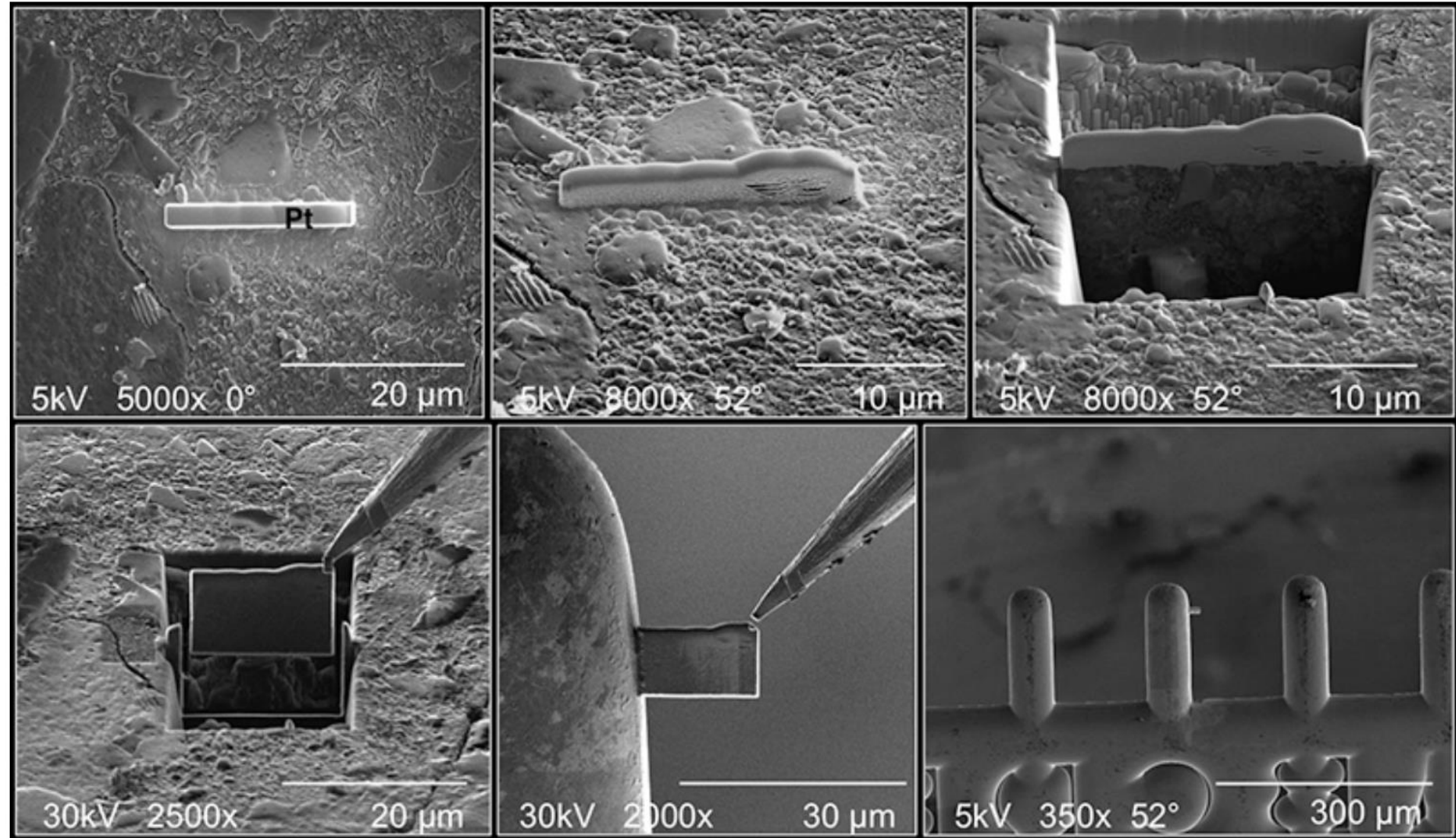


<https://www.imri.uci.edu/content/fei-quanta-3d-feg-dual-beam-semfib-0>



Field Emission
Electron
Microscopy
FIB

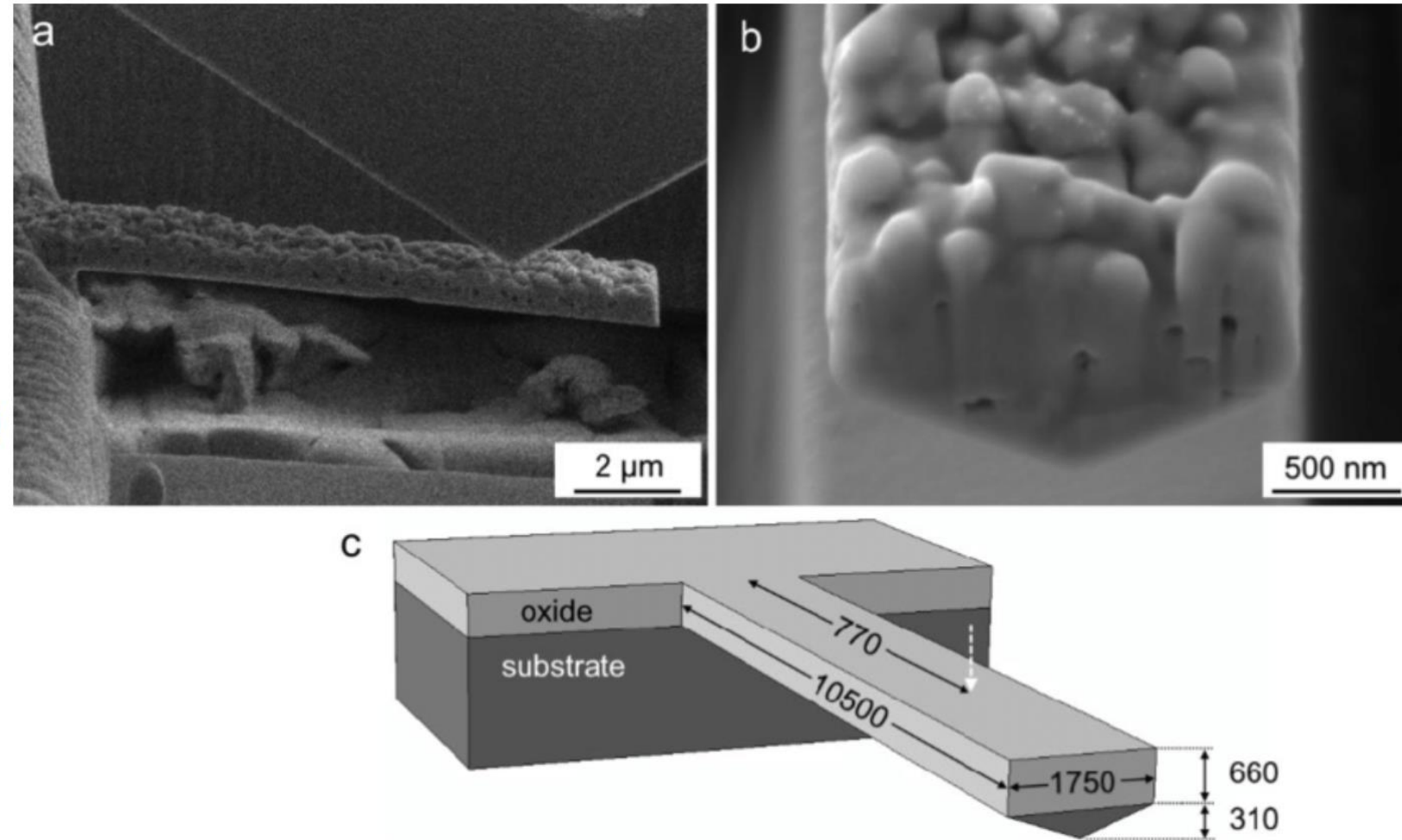
http://www.soest.hawaii.edu/AEMC/instruments/aemc_helios.htm



FIB preparation of an electron-transparent thin section of a meteorite sample.



Field Emission
Electron
Microscopy
FIB



SEM images of FIB milled cantilever, showing (a) side view during bending test and (b) front view prior to test (sample tilted at 55° with respect to horizontal axis); (c) Model for FE simulation (dimensions in nm)



EBSD

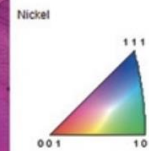
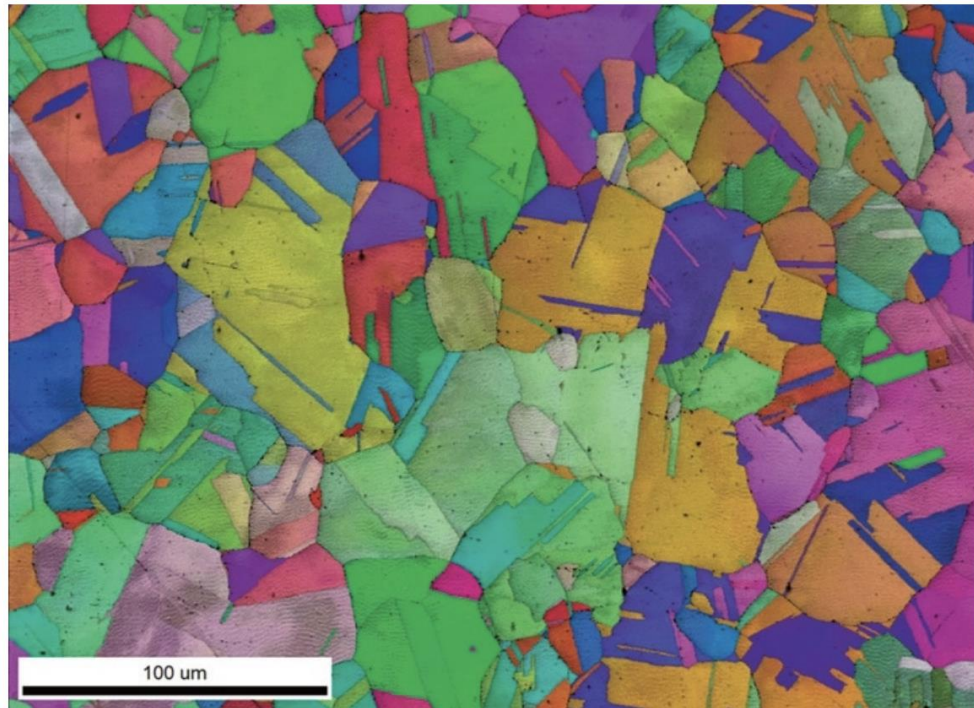


Figure 1. EBSD IQ + IPF map from a Ni superalloy collected at 3,000 indexed points per second at 11 nA with 99.6% indexing success.

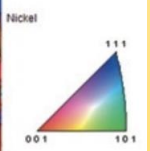
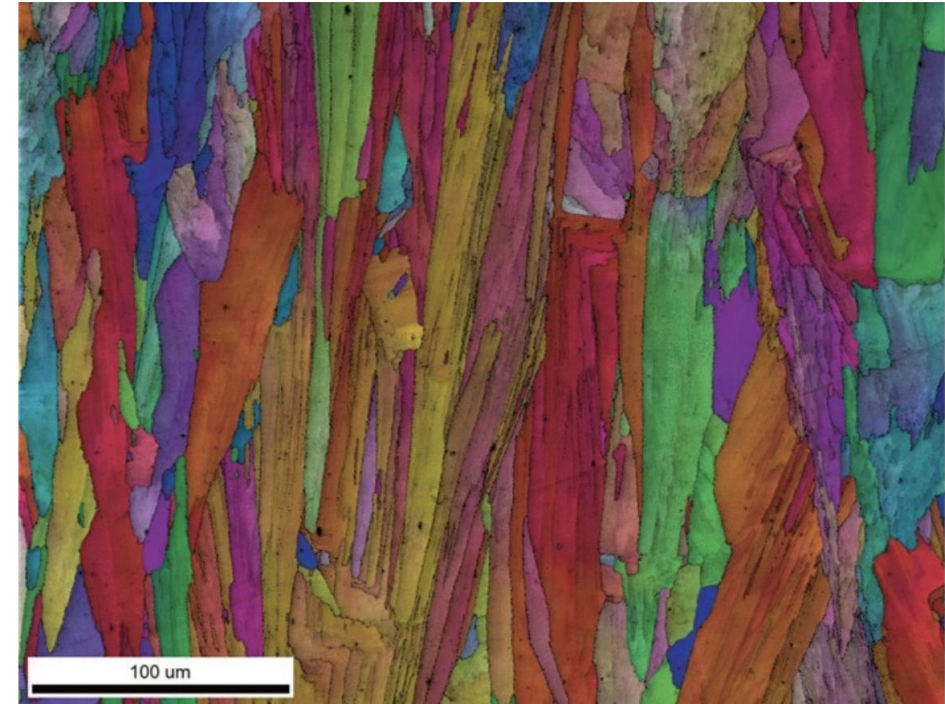


Figure 2. EBSD IQ + IPF map from an additively manufactured IN718 alloy collected at 4,500 indexed points per second.

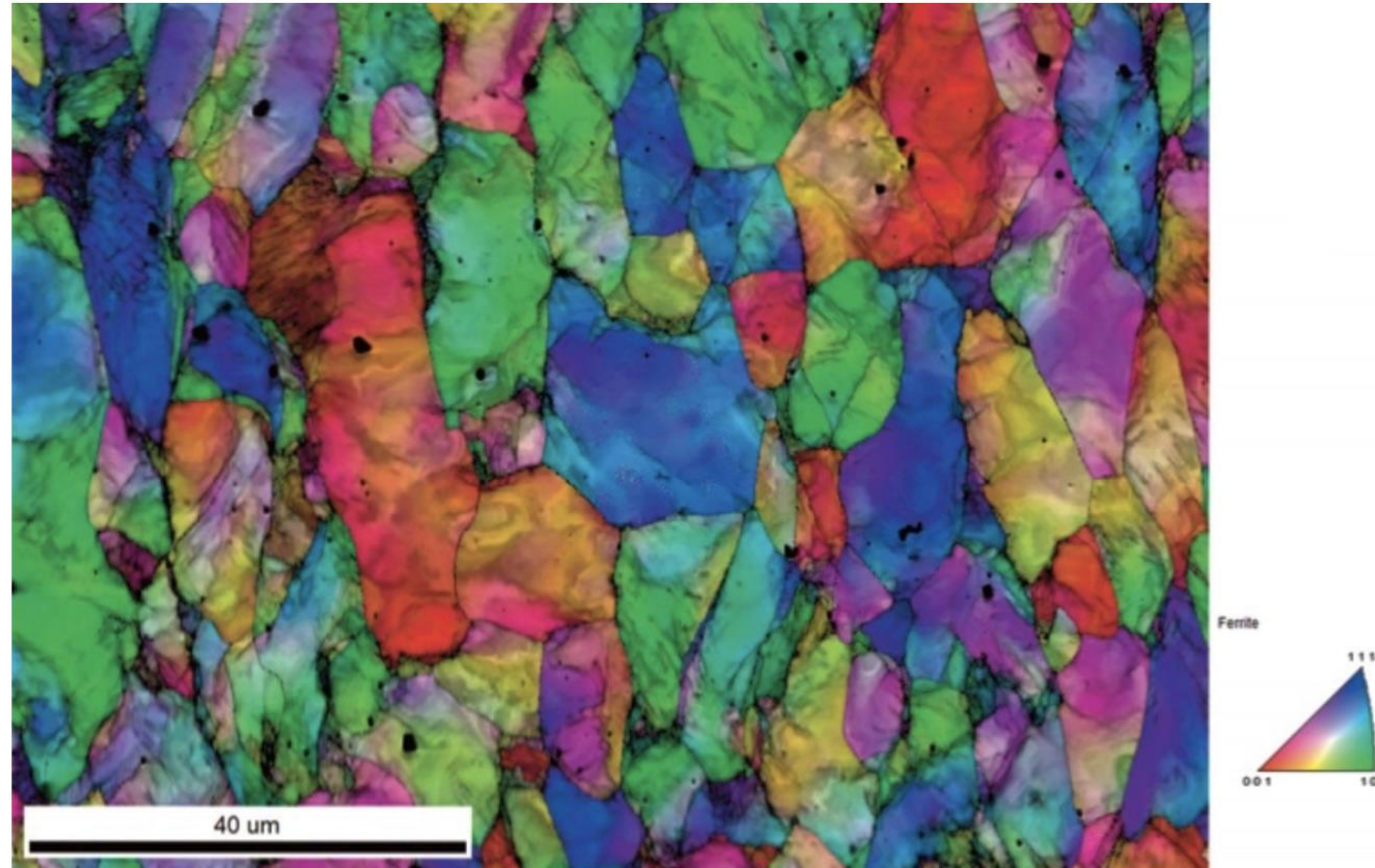
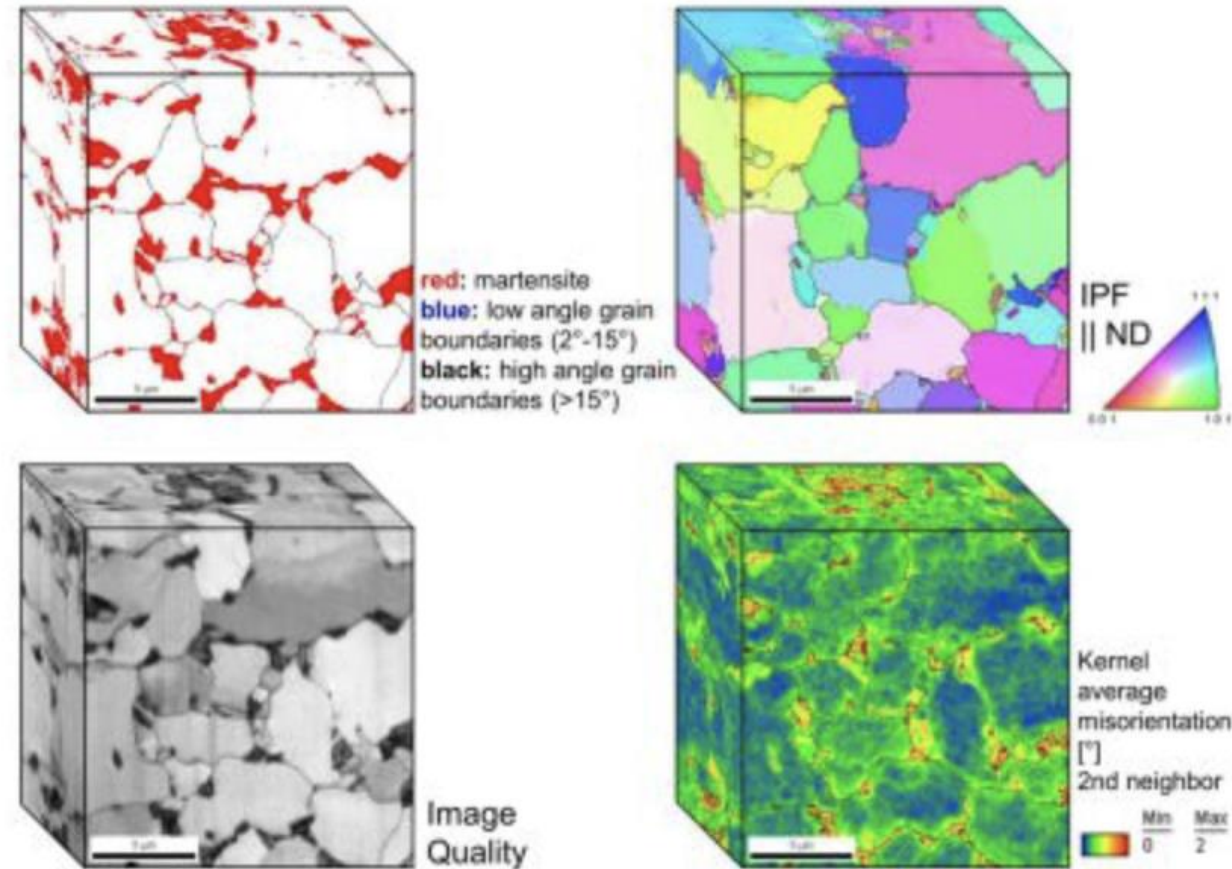
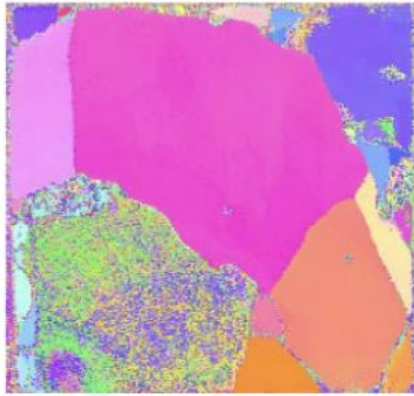


Figure 3. EBSD IQ + IPF map from a deformed ferritic steel sample.

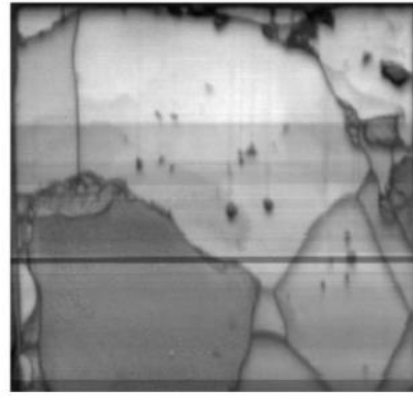


Dual phase steel microstructure revealed by 3D EBSD.

<http://www.dierk-raabe.com/ebsd-and-3d-ebsd/>



(a)



(b)

FIGURE 7. (a) IPF showing inability to assess local orientation texture for HfAl_3 grains, (b) greyscale image showing overall grain structure.

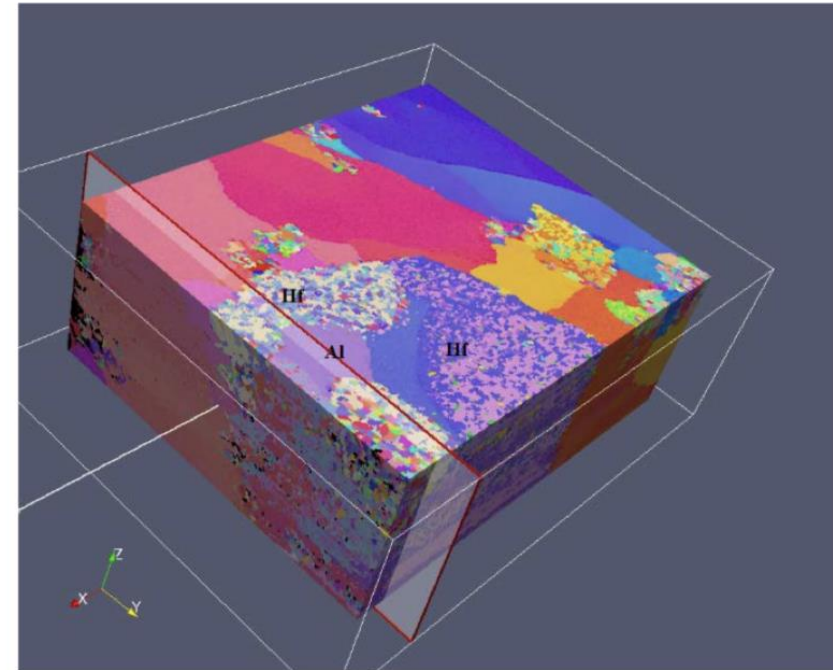


FIGURE 10. The 3D reconstruction model to show the Al grain surrounded by HfAl_3 grains.

Transmission Electron Microscopy - TEM



In Transmission Electron Microscopy (TEM) a thin solid specimen (**5** 200 nm thick) is bombarded in vacuum with a highly-focused, monoenergetic beam of electrons. The beam is of sufficient energy to propagate through the specimen. A series of electromagnetic lenses then magnifies this transmitted electron signal. Diffracted electrons are observed in the form of a diffraction pattern beneath the specimen. This information is used to determine the atomic structure of the material in the sample. Transmitted electrons form images from small regions of sample that contain contrast, due to several scattering mechanisms associated with interactions between electrons and the atomic constituents of the sample. Analysis of transmitted electron images yields information both about atomic structure and about defects present in the ma

Range of elements	TEM does not specifically identify elements measured
Destructive	Yes, during specimen preparation
Chemical bonding information	Sometimes, indirectly from diffraction and image simulation
Quantification	Yes, atomic structures by diffraction; defect characterization by systematic image analysis
Accuracy	Lattice parameters to four significant figures using convergent beam diffraction
Detection limits	One monolayer for relatively high- <i>Z</i> materials
Depth resolution	None, except there are techniques that measure sample thickness
Lateral resolution	Better than 0.2 nm on some instruments
Imaging/mapping	Yes
Sample requirements	Solid conductors and coated insulators. Typically 3-mm diameter, < 200-nm thick in the center
Main uses	Atomic structure and Microstructural analysis of solid materials, providing high lateral resolution
Instrument cost	\$300,000–\$1,500,000
Size	100 ft. ² to a major lab

Transmission Electron Microscopy - TEM

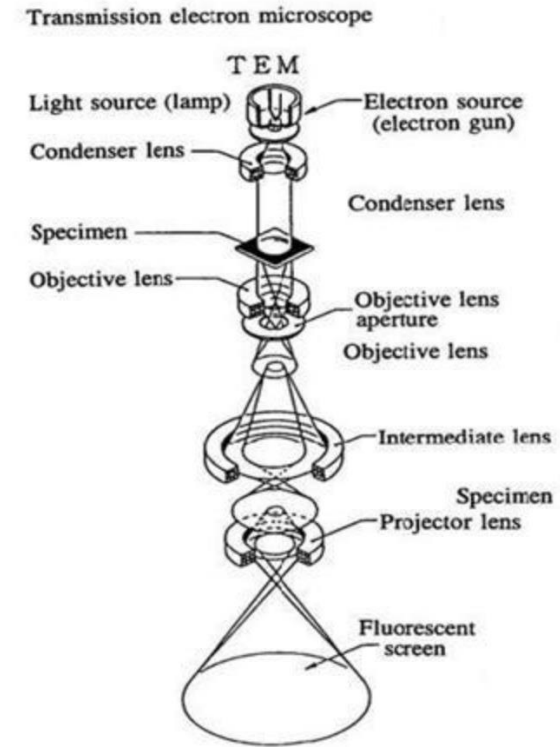
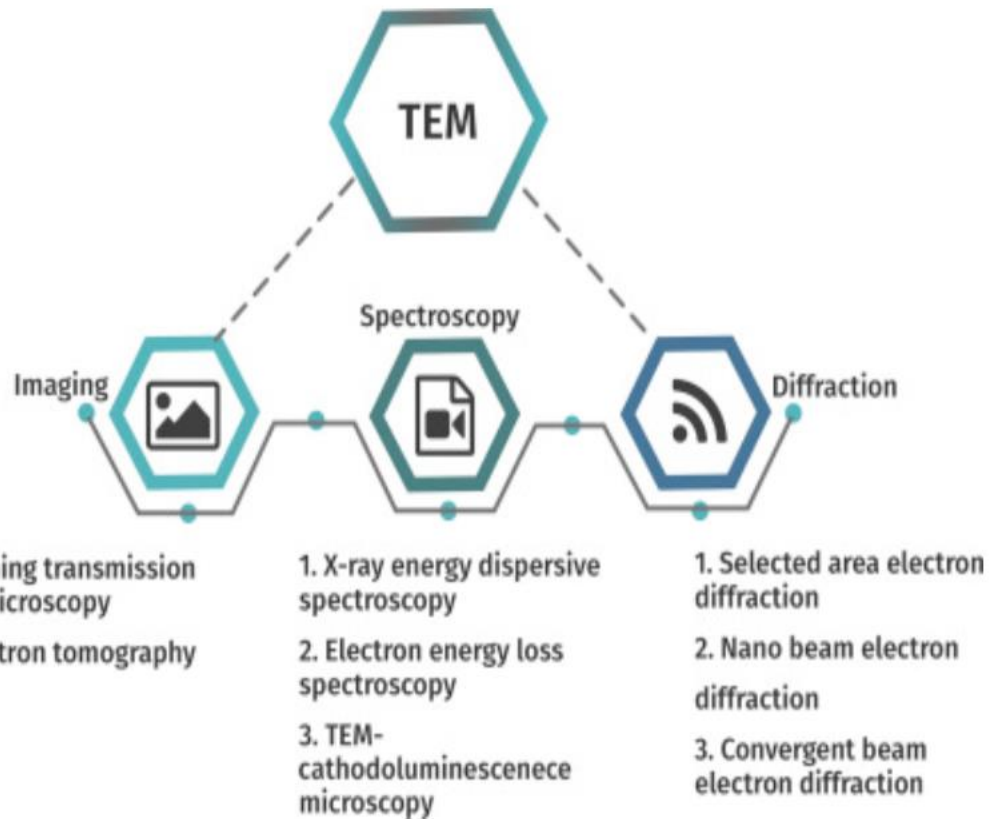


Fig 1

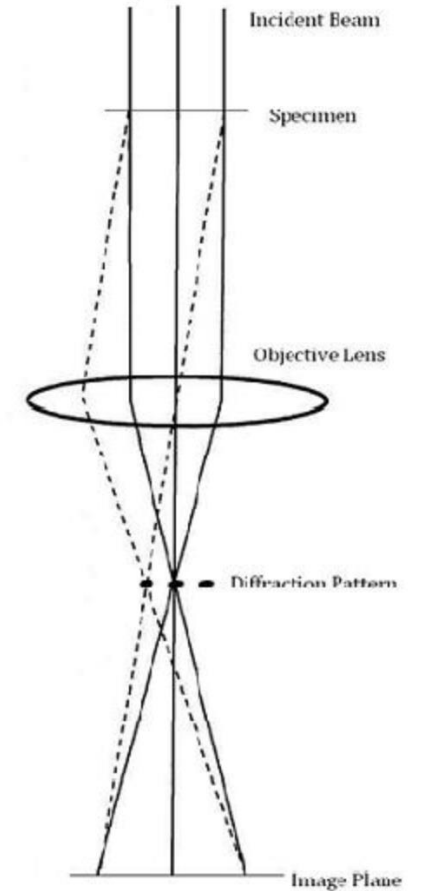
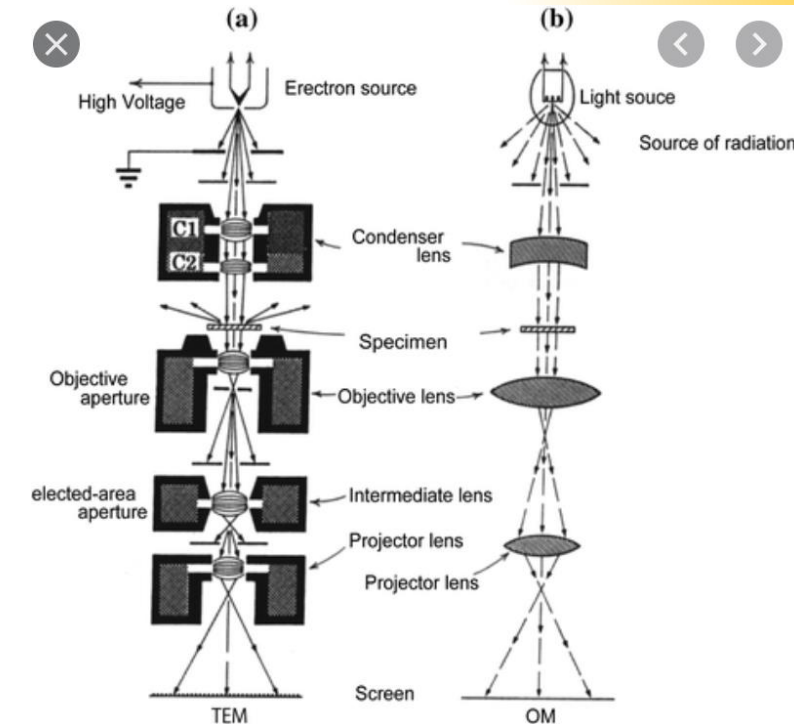
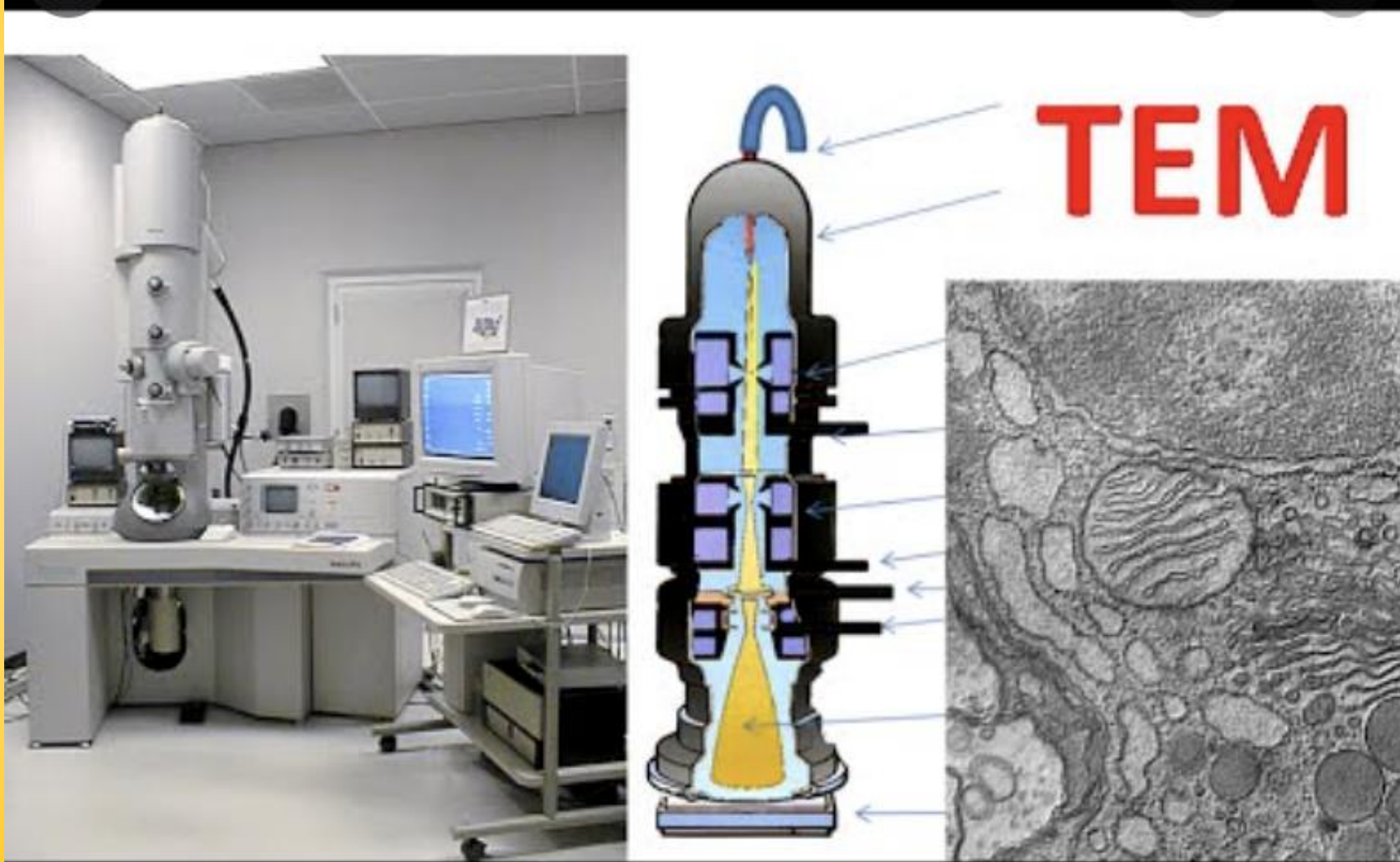


Fig 2

<https://www.sciencedirect.com/topics/materials-science/transmission-electron-microscopy>

Fig 1 - General layout of a TEM describing the path of electron beam in a TEM (Taken from JEOL 2000FX Handbook)

Fig 2 - A ray diagram for the diffraction mechanism in TEM



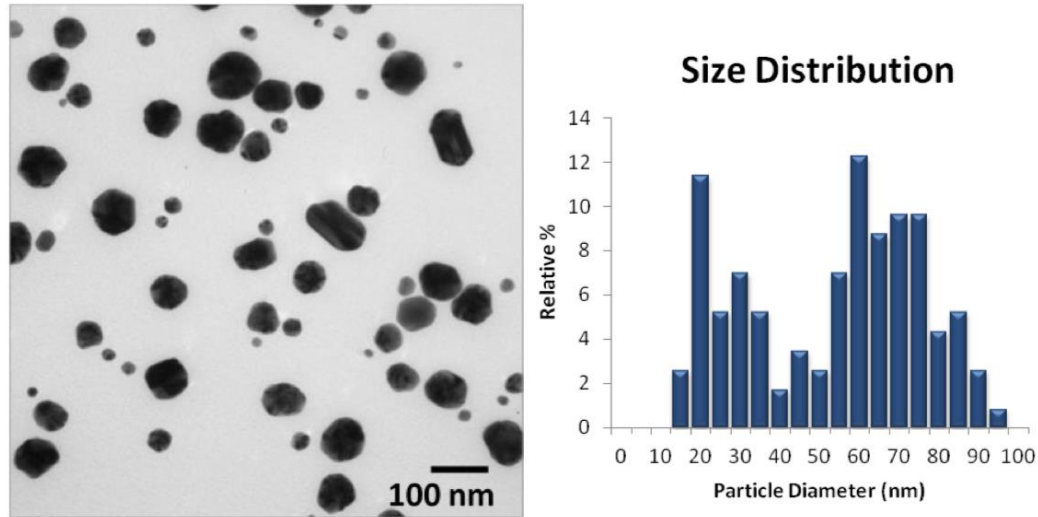
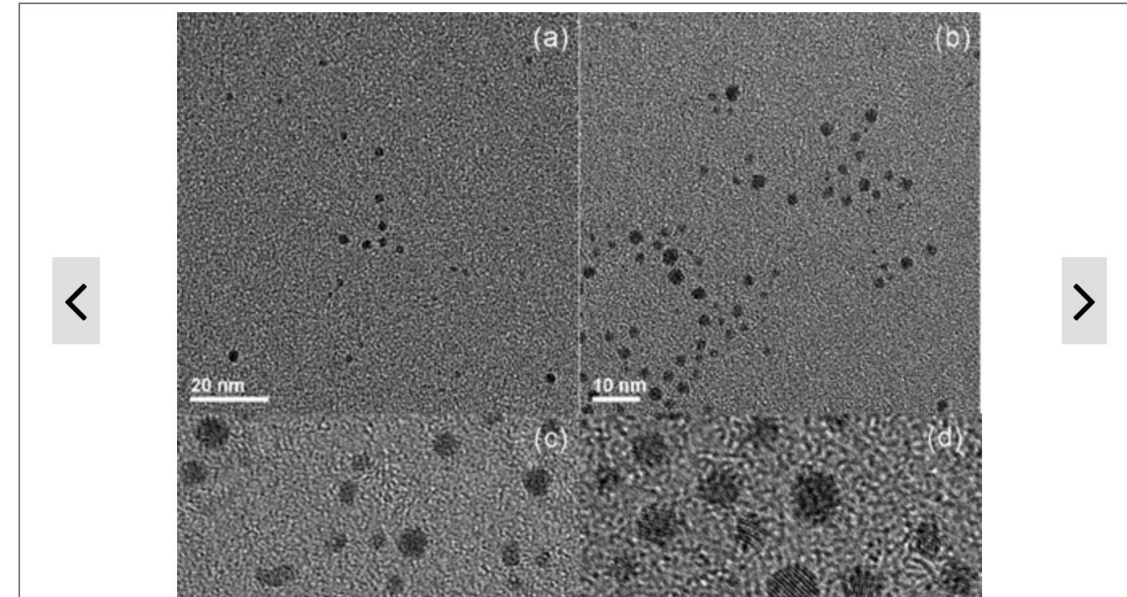


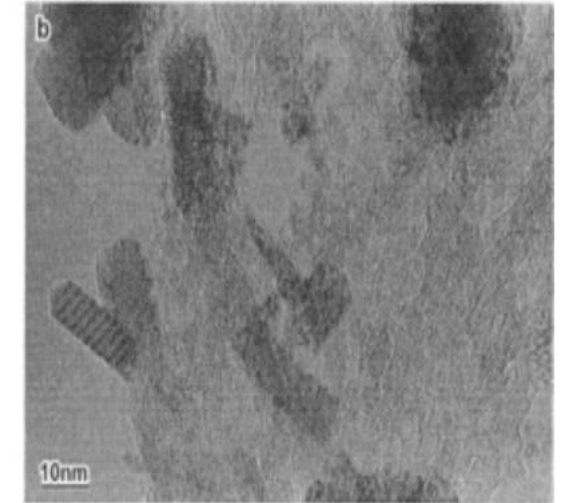
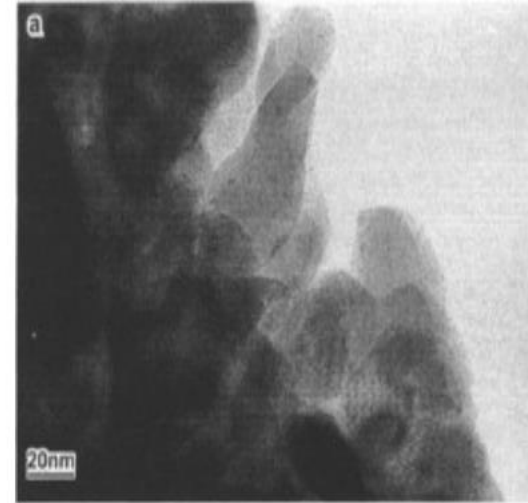
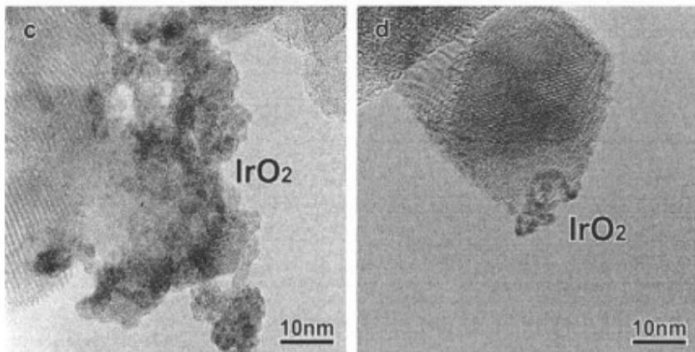
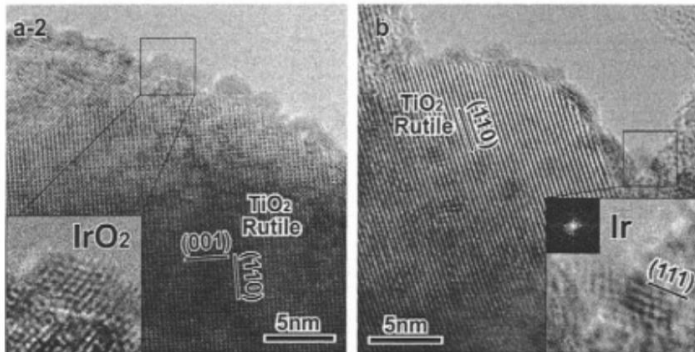
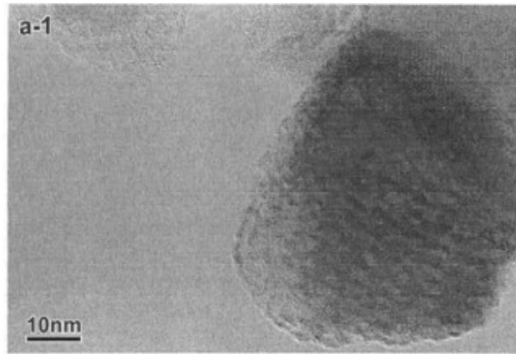
Figure 3. For particles that are size and shape polydisperse, a size distribution can be obtained by measuring each particle diameter at a fixed angle. The random orientation of particles allows for a statistical measure of the size distribution to be generated.



 [Download Hi-Res Image](#) |  [Download to MS-PowerPoint](#)

 [Cite This: *Langmuir* 2008, 24, 20, 11350-11360](#)

<http://50.87.149.212/sites/default/files/nanoComposix%20Guidelines%20for%20TEM%20Analysis.pdf>



[Download full-size image](#)

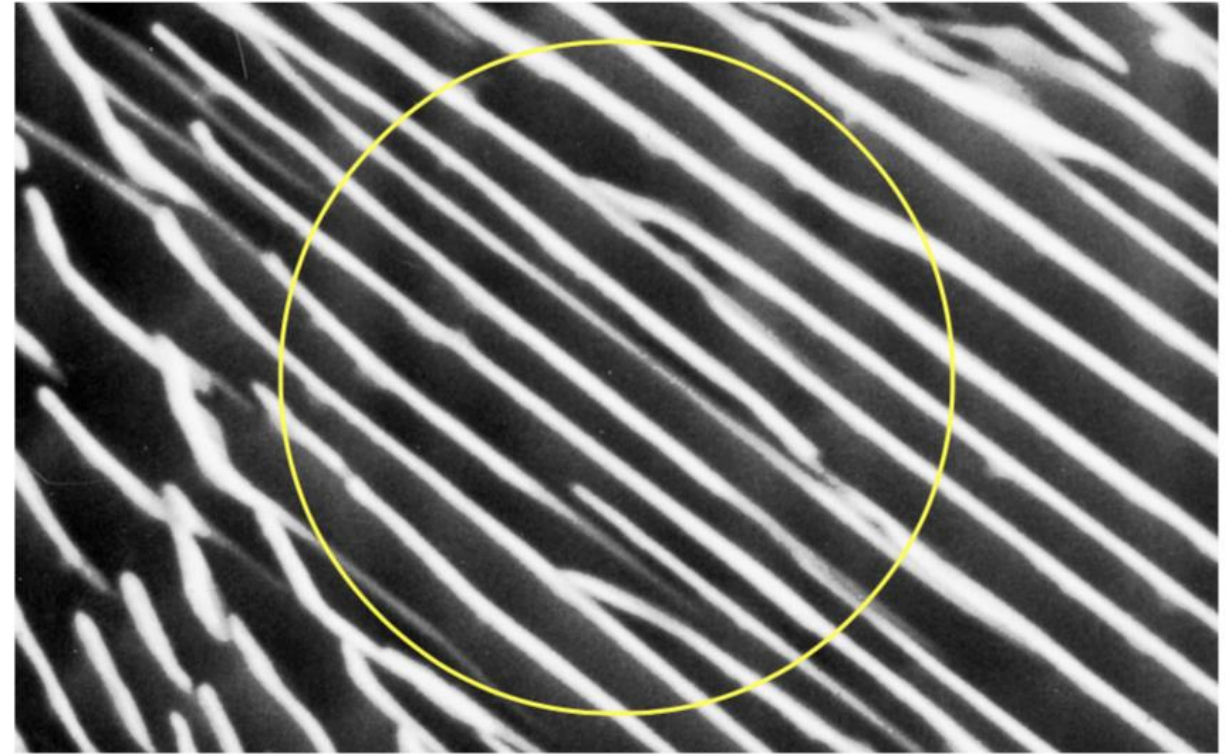
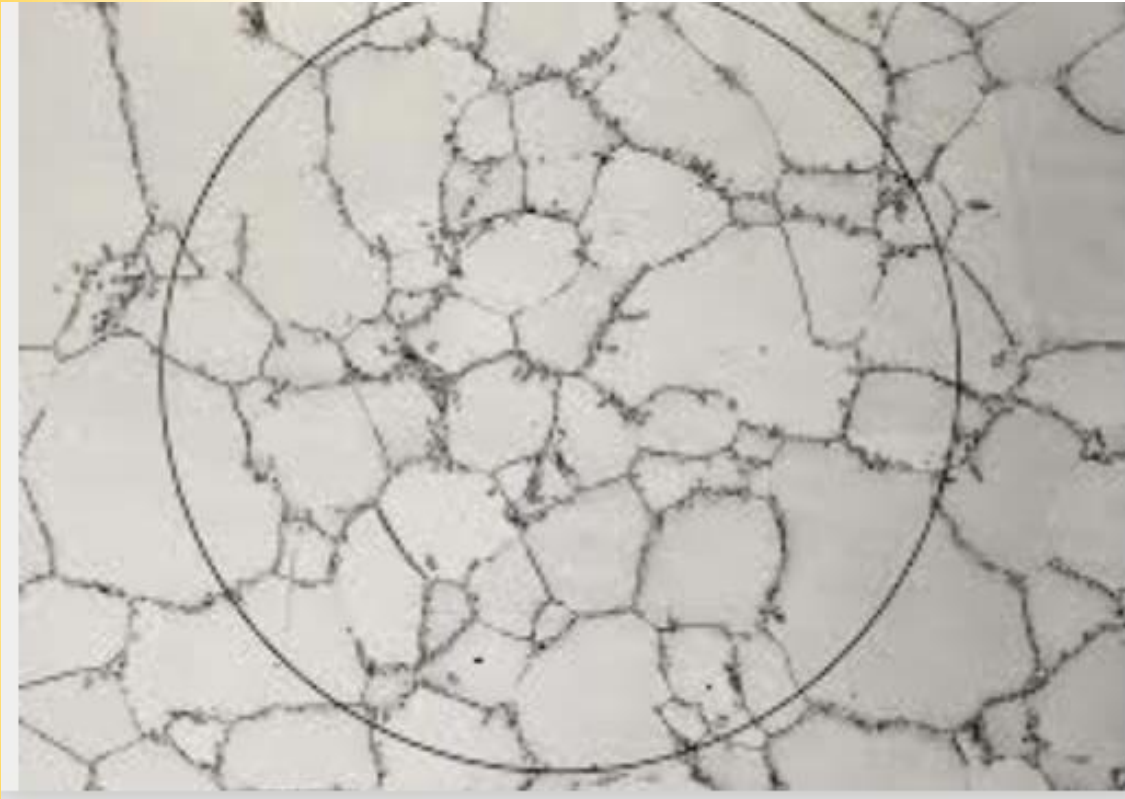
Fig. 4. (a) TEM image of Ir/Fe₂O₃ prepared by DP and (b) TEM image of Ir/Al₂O₃ prepared by DP.

Fig. 5. TEM images of the Ir/TiO₂ catalysts prepared by the DP method followed by the pretreatment at 523 K (a-1) prepared at pH 8 and calcined in air, (a-2) prepared at pH 8 and calcined in air, (b) prepared at pH 8 and calcined in the hydrogen stream, (c) prepared at pH 3 and calcined in air, (d) prepared at pH 5 and calcined in air.

<https://www.sciencedirect.com/topics/chemistry/tem-image>

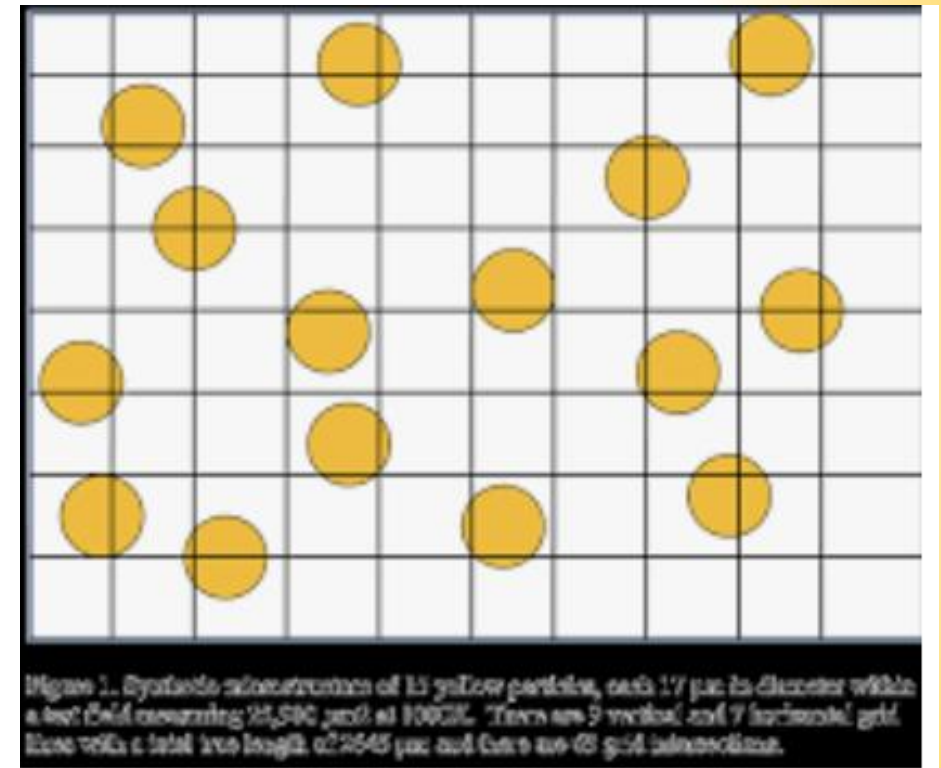
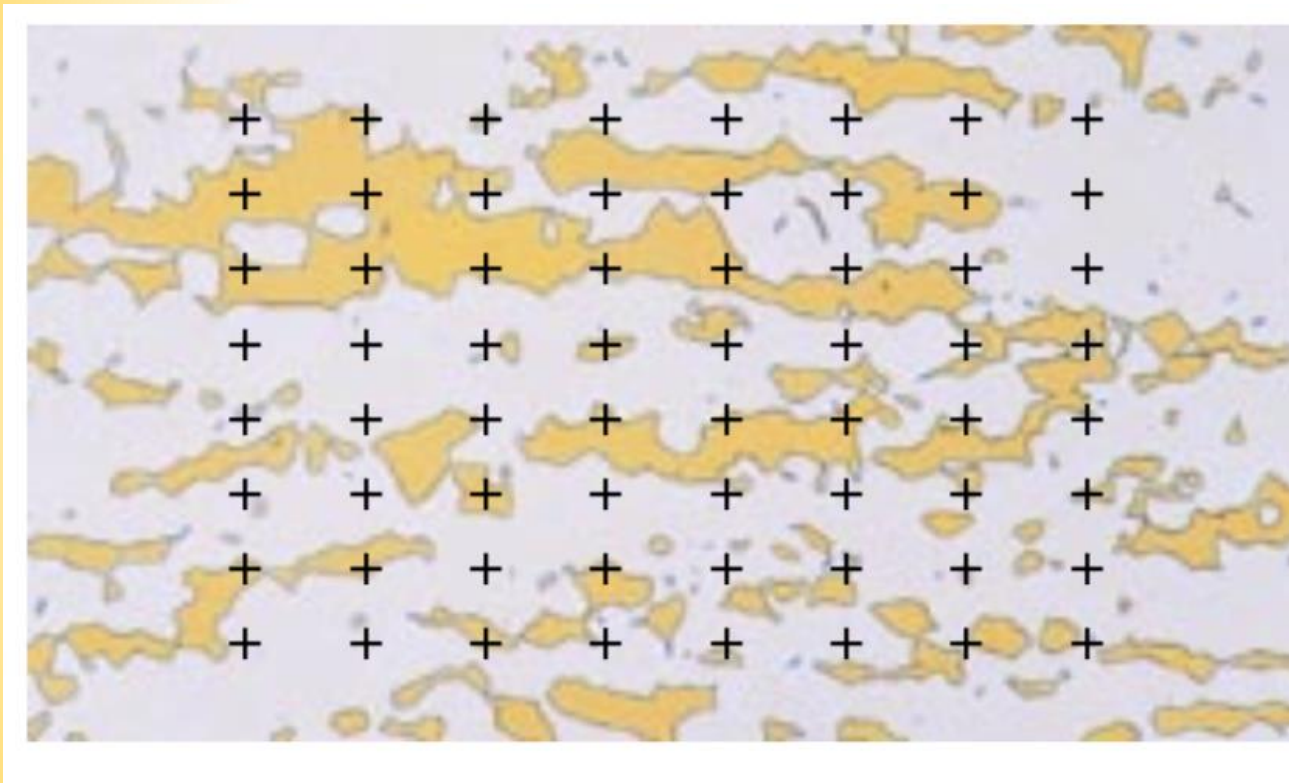


Quantitative Metallography





Quantitative Metallography

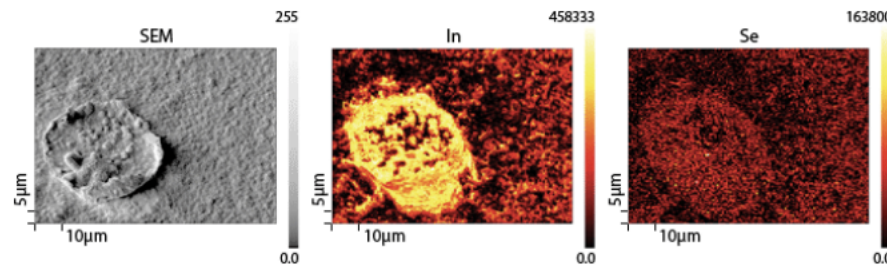


Introduction to Quantitative Metallography
George Vander Voort



Auger

Field Emission Auger Electron Spectroscopy with Scanning Auger Microscopy



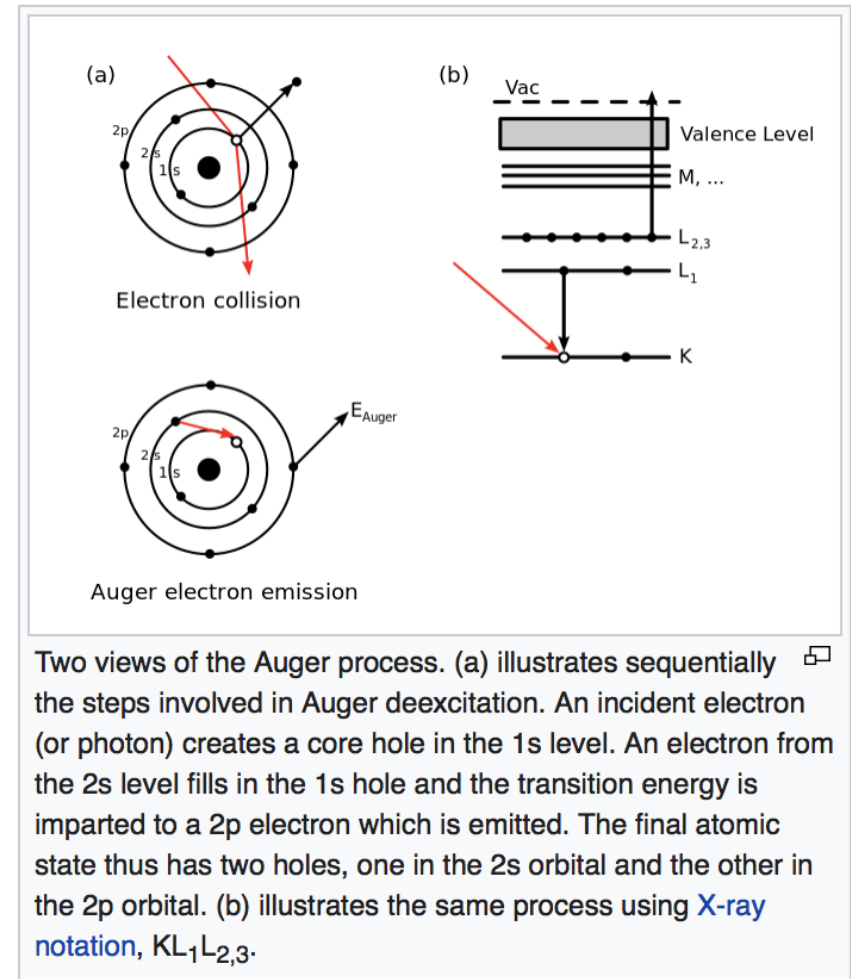
(a) SEM and (b&c) SAM images of a surface defect in Cu(In,Ga)SeS. SAM analysis shows the defect to be an In-rich region (b), indicating that the likely origin was an "In-spit" during precursor deposition that was subsequently selenized during downstream processing (c).

In Auger electron spectroscopy (AES), we bombard a sample surface with a focused beam of high-energy (2- to 10-kV) electrons. The incident electrons lose energy to the sample atoms, generating Auger electrons that have discrete kinetic energies characteristic of the emitting atoms.

<https://www.nrel.gov/materials-science/auger-electron.html>



The **Auger effect** is a physical phenomenon in which the filling of an inner-shell vacancy of an atom is accompanied by the emission of an electron from the same atom.^[1] When a core electron is removed, leaving a vacancy, an electron from a higher energy level may fall into the vacancy, resulting in a release of energy. Although most often this energy is released in the form of an emitted photon, the energy can also be transferred to another electron, which is ejected from the atom; this second ejected electron is called an **Auger electron**.

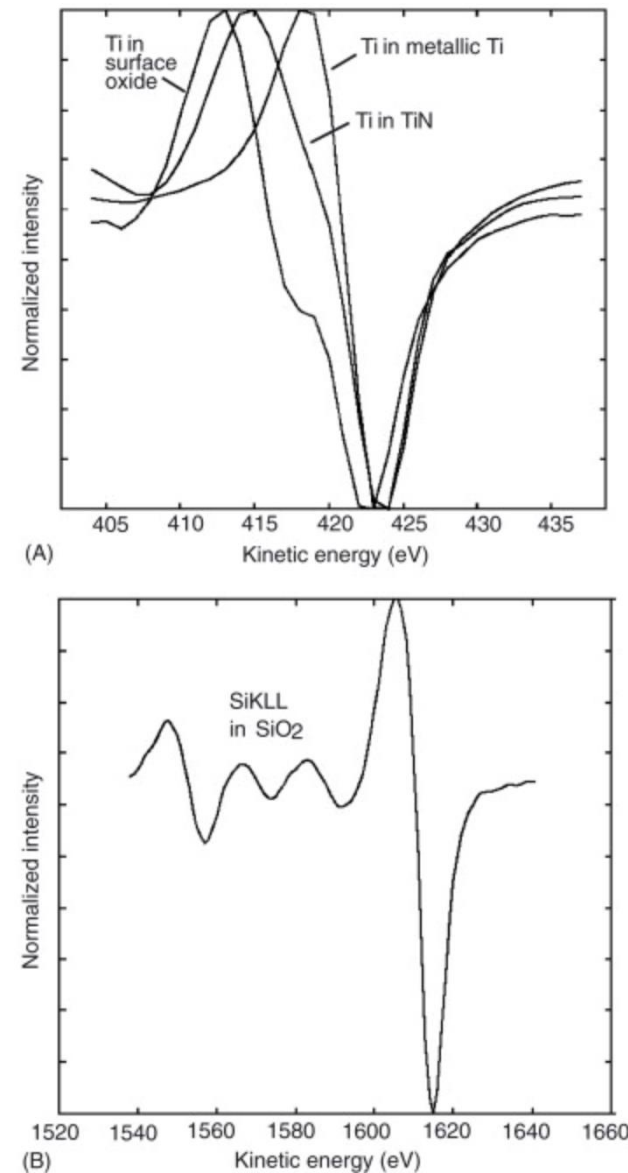


Auger electron spectroscopy involves the emission of Auger electrons by bombarding a sample with either X-rays or energetic electrons and measures the intensity of Auger electrons that result as a function of the Auger electron energy. The resulting spectra can be used to determine the identity of the emitting atoms and some information about their environment.



<https://www.sciencedirect.com/topics/medicine-and-dentistry/auger-electron-spectroscopy>

Auger



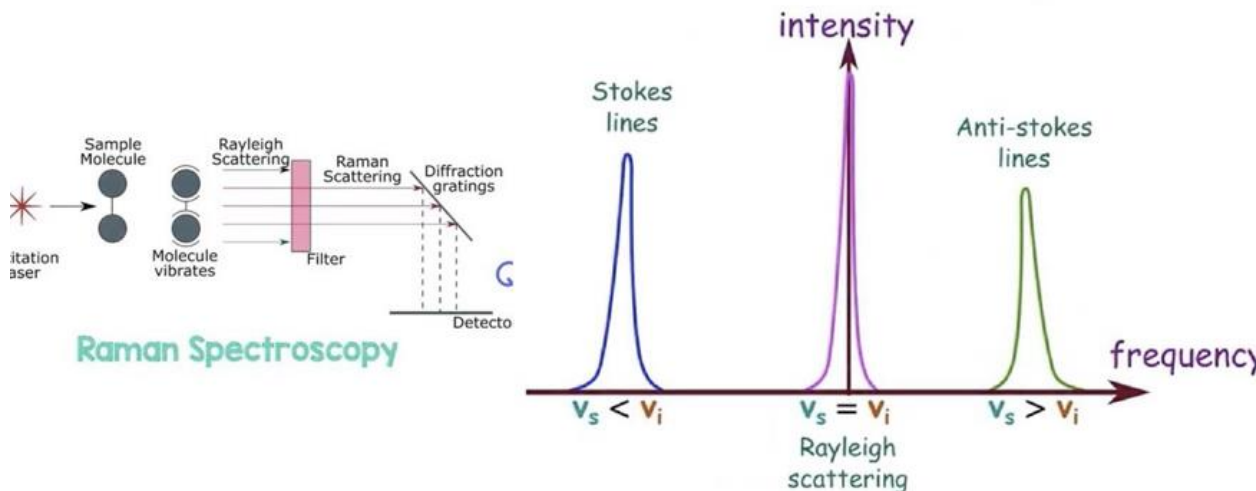
[Download full-size image](#)

Figure 7. (A) Ti $L_{3}M_{23}V$ $d(N(E) \times E)/dE$ Auger spectra of a Ti surface oxide, TiN, and metallic Ti. (B) Si KLL $d(N(E) \times E)/dE$ Auger spectra of silicon dioxide. (Reproduced with permission from ULVAC-PHI.)



Raman Spectroscopy

Basics and Principles



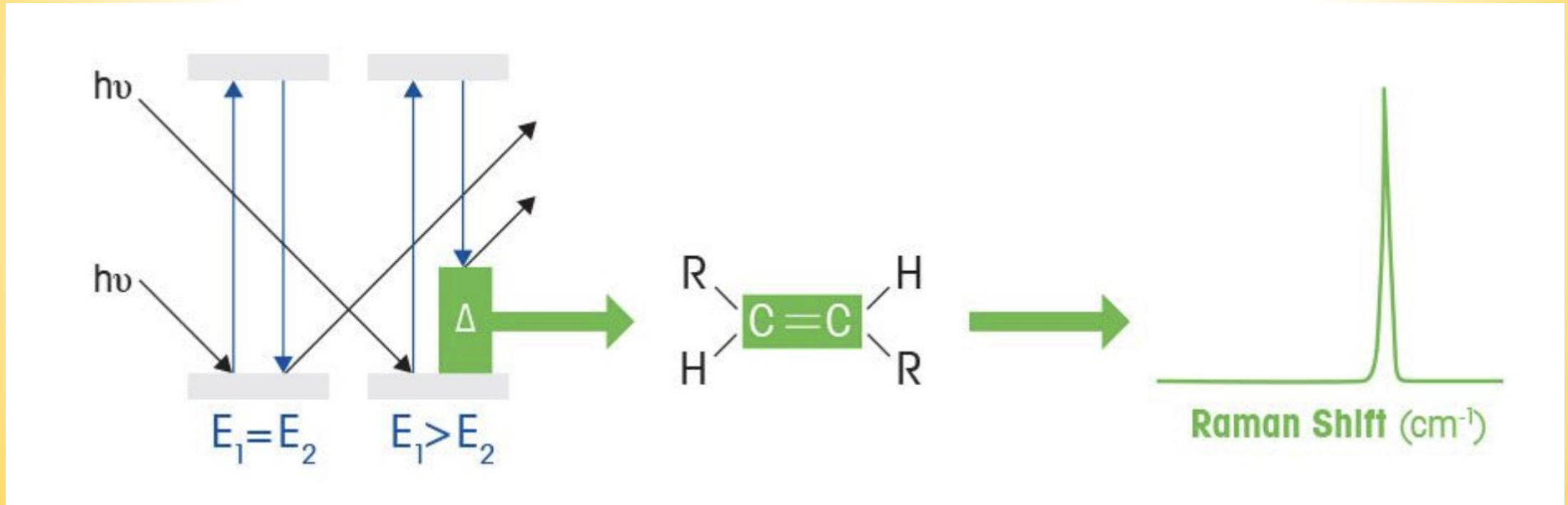
The diagram illustrates the Raman spectroscopy process. An excitation laser beam passes through a sample molecule, causing it to vibrate. This results in three types of scattering: Rayleigh Scattering (where the scattered light has the same frequency as the incident light), Raman Scattering (Stokes lines, where the scattered light has a lower frequency), and Raman Scattering (Anti-stokes lines, where the scattered light has a higher frequency). The setup includes a filter to remove the Rayleigh scattering, diffraction gratings to separate the Raman lines, and a detector to measure the intensity.

The spectrum shows intensity versus frequency. The Stokes lines are at a lower frequency ($\nu_s < \nu_i$), the Rayleigh scattering is at the same frequency ($\nu_s = \nu_i$), and the Anti-stokes lines are at a higher frequency ($\nu_s > \nu_i$).

https://www.mt.com/br/pt/home/applications/L1_AutoChem_Applications/Raman-Spectroscopy.html



Raman spectroscopy is a **spectroscopic** technique typically used to determine vibrational modes of molecules, although rotational and other low-frequency modes of systems may also be observed.

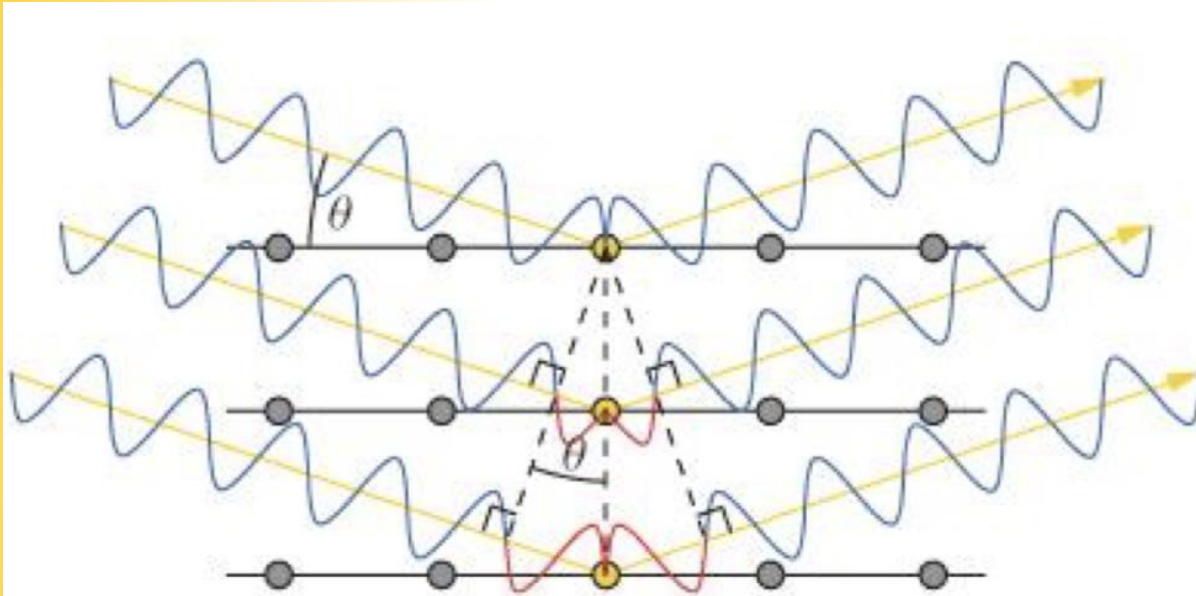


https://www.mt.com/br/pt/home/applications/L1_AutoChem_Applications/Raman-Spectroscopy.html

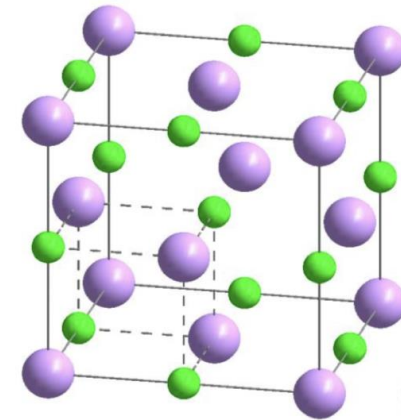


X-Ray Diffraction

Lei de Bragg



$$2d\sin\theta = n\lambda$$



NaCl – fcc lattice

Fm-3m
a = 5.64 Å

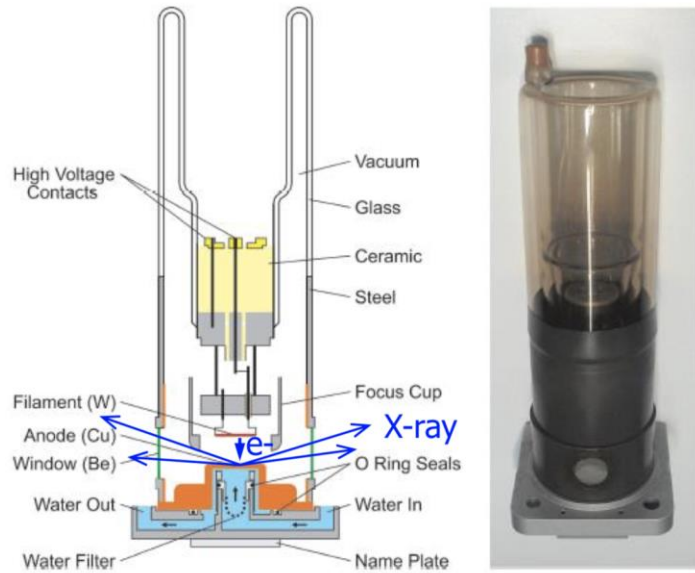
Bragg:

In sodium chloride there appear to be no molecules represented by NaCl. The equality in number of sodium and chloride atoms is arrived at by a chess-board pattern of these atoms; it is a result of geometry and not of a pairing off of the atoms



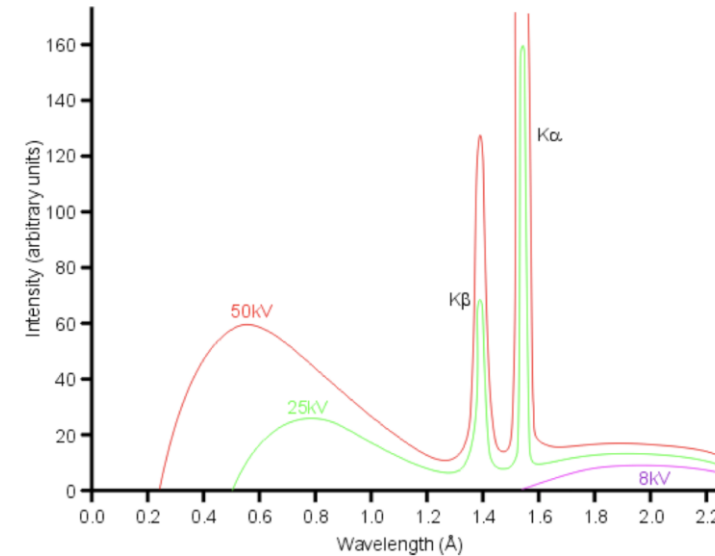
X-Ray Diffraction

Conventional X-ray laboratory source



Electrostatic potential 20 to 60 kV
 Anode current 10 to 50 mA
 Input power ~ 0.5 to 3 kW
 Only 0.1% transforms into X-ray beam
 The wavelengths, most commonly used in crystallography: 0.5-2.5 Å

A typical x-ray spectrum from a Cu target



$$eV = h\nu = \frac{hc}{\lambda}$$

$$\lambda_c = \frac{12.4}{V, kV} \text{ \AA}$$

http://www.fhi-berlin.mpg.de/acnew/departament/pages/teaching/pages/teaching__wintersemester__2014_2015/elena_willinger__fundamental_of_x-ray_diffraction__141107.pdf



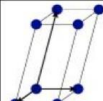
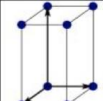
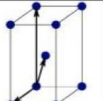
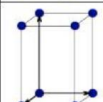
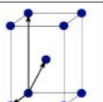
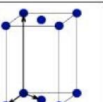
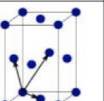
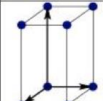
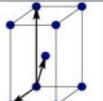
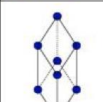
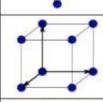
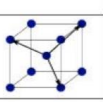
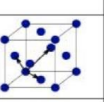
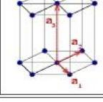
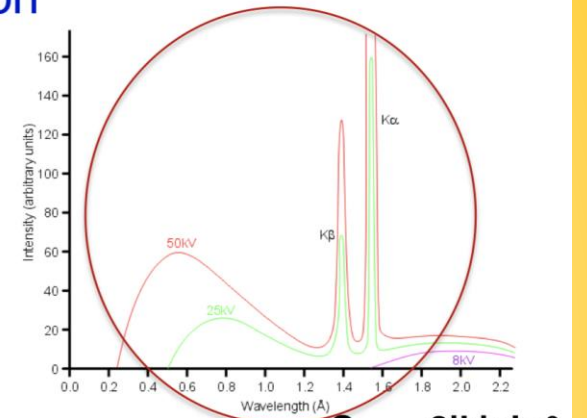
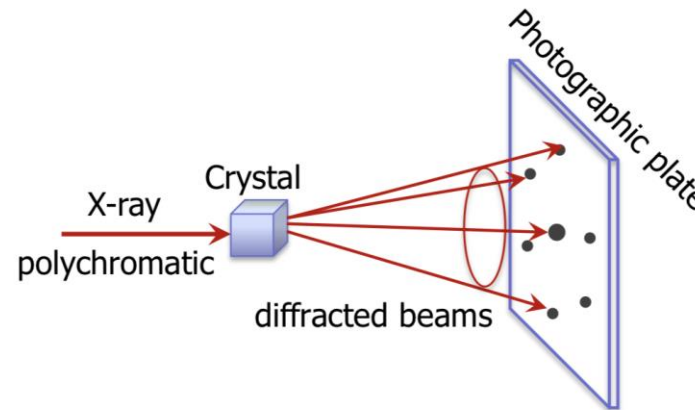
Bravais lattice	Parameters	Simple (P)	Volume centered (I)	Base centered (C)	Face centered (F)
Triclinic	$a_1 \neq a_2 \neq a_3$ $\alpha_{12} \neq \alpha_{23} \neq \alpha_{31}$				
Monoclinic	$a_1 \neq a_2 \neq a_3$ $\alpha_{23} = \alpha_{31} = 90^\circ$ $\alpha_{12} \neq 90^\circ$				
Orthorhombic	$a_1 \neq a_2 \neq a_3$ $\alpha_{12} = \alpha_{23} = \alpha_{31} = 90^\circ$				
Tetragonal	$a_1 = a_2 \neq a_3$ $\alpha_{12} = \alpha_{23} = \alpha_{31} = 90^\circ$				
Trigonal	$a_1 = a_2 = a_3$ $\alpha_{12} = \alpha_{23} = \alpha_{31} < 120^\circ$				
Cubic	$a_1 = a_2 = a_3$ $\alpha_{12} = \alpha_{23} = \alpha_{31} = 90^\circ$				
Hexagonal	$a_1 = a_2 \neq a_3$ $\alpha_{12} = 120^\circ$ $\alpha_{23} = \alpha_{31} = 90^\circ$				

Table 1.1: Bravais lattices in three-dimensions.

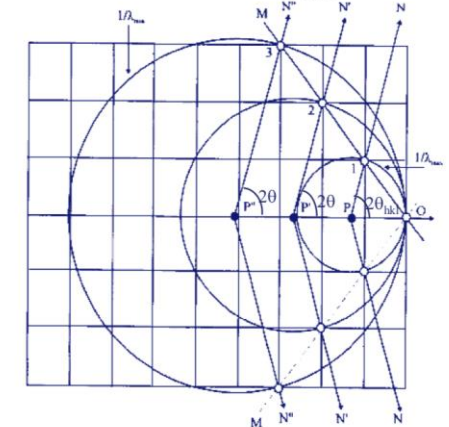
Laue diffraction

$$2d_{hkl} \sin \theta_{hkl} = \lambda$$

θ_{hkl} is fixed \longrightarrow polychromatic radiation
The crystal position is fixed



$$G_{hkl} = 2kl \sin \theta$$



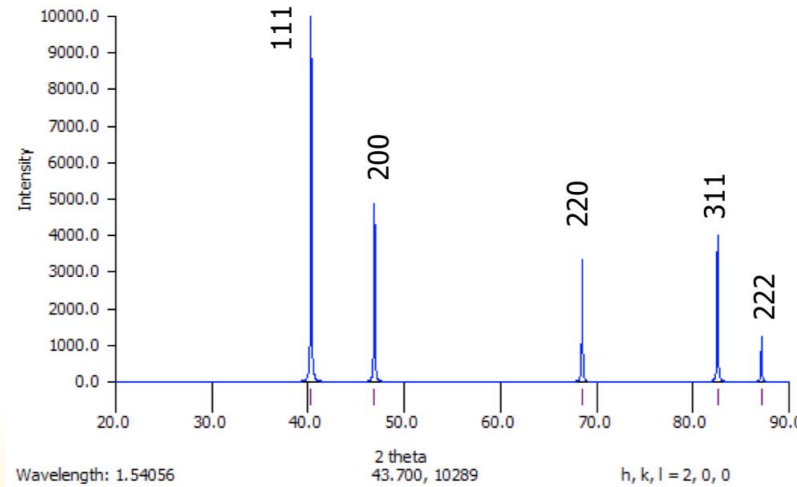
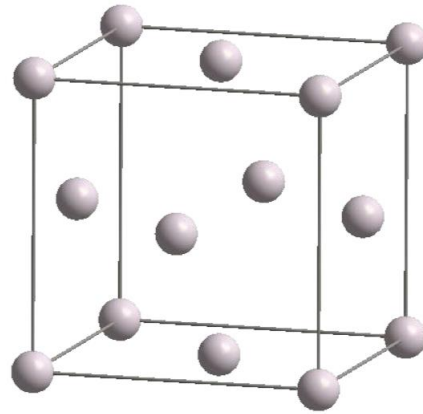


X-Ray Diffraction

http://www.fhi-berlin.mpg.de/acnew/department/pages/teaching/pages/teaching_wintersemester_2014_2015/elena_willinger_fundamental_of_x-ray_diffraction_141107.pdf

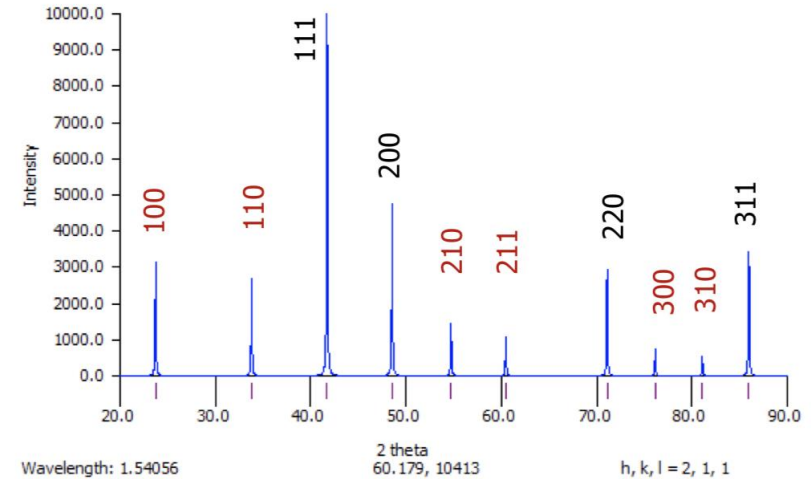
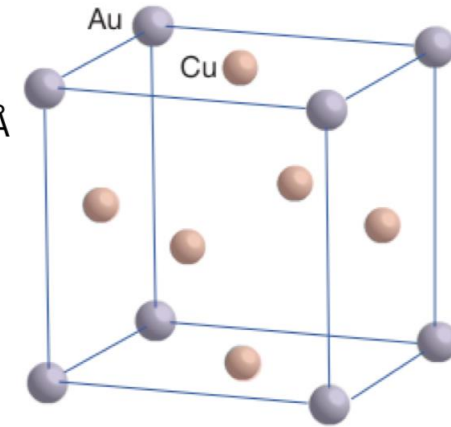
AuCu- face-centred cubic (F), fcc
disordered solid solution

Fm-3m
a= 3.872 Å



AuCu₃- primitive cubic (P)
ordered solid solution

Pm-3m
a= 3.747 Å



X-Ray Diffraction



Aeris



Benchtop X-ray diffractometer

[More details >](#)

Empyrean range



Multipurpose X-ray diffractometers for your analytical needs

[More details >](#)

X'Pert³ MRD



Versatile research & development XRD system

[More details >](#)

X'Pert³ MRD XL



Versatile research, development & quality control XRD system

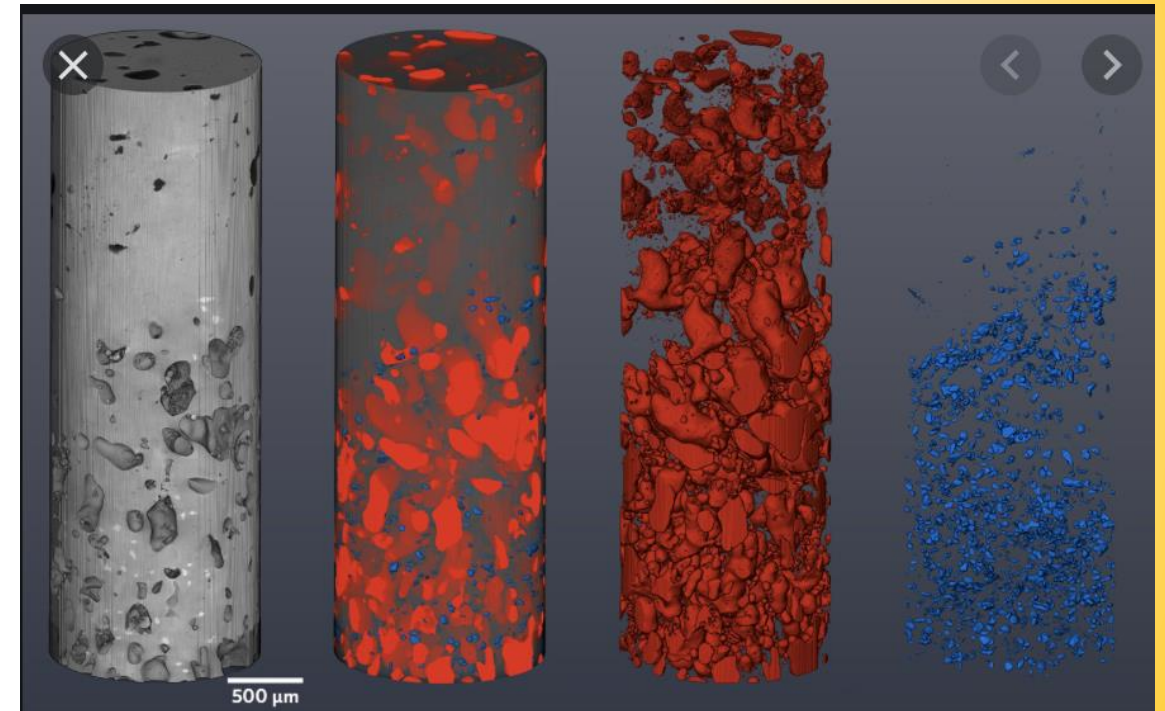
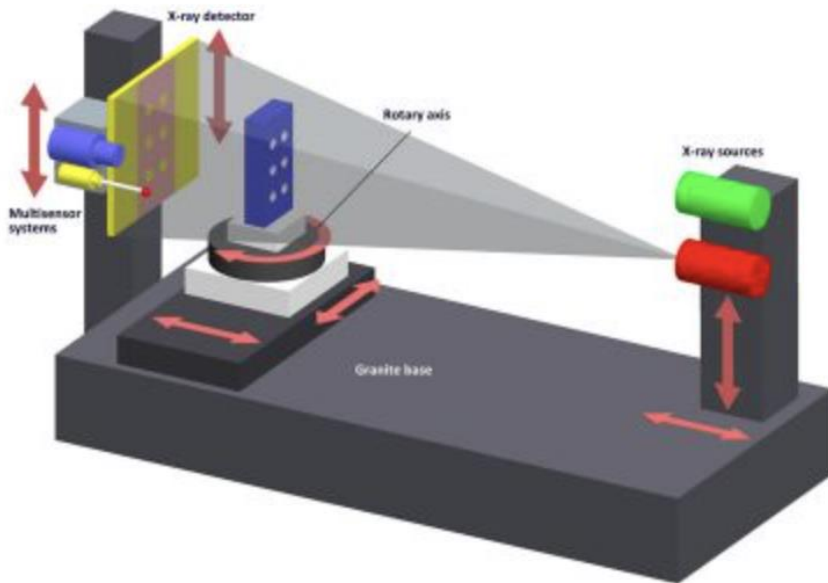
[More details >](#)

Technology				
X-ray Diffraction (XRD)	✓	✓	✓	✓
Measurement type				
Particle shape		✓		
Particle size		✓		
Crystal structure determination	✓	✓		
Phase identification	✓	✓	✓	✓
Phase quantification	✓	✓	✓	✓
Contaminant detection and anal...		✓		
Epitaxy analysis		✓	✓	✓
Interface roughness		✓	✓	✓
3D structure / imaging		✓		
Thin film metrology		✓	✓	✓
Residual stress		✓	✓	✓



X-Ray Tomography

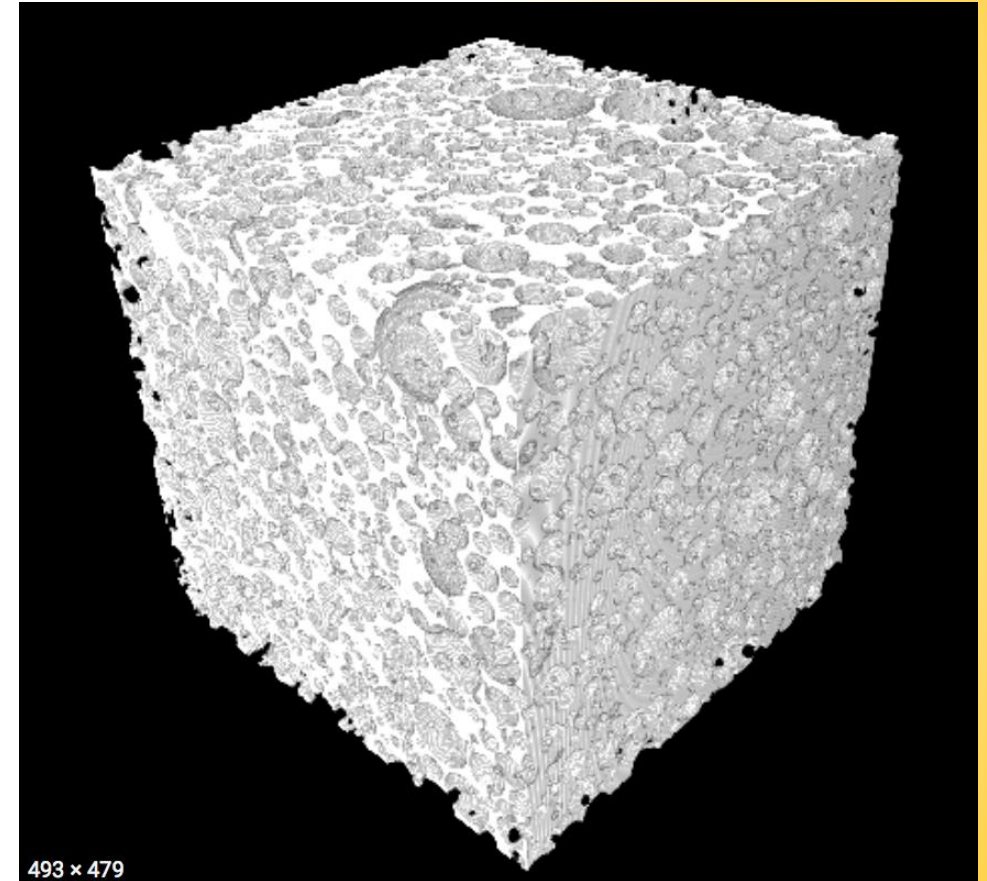
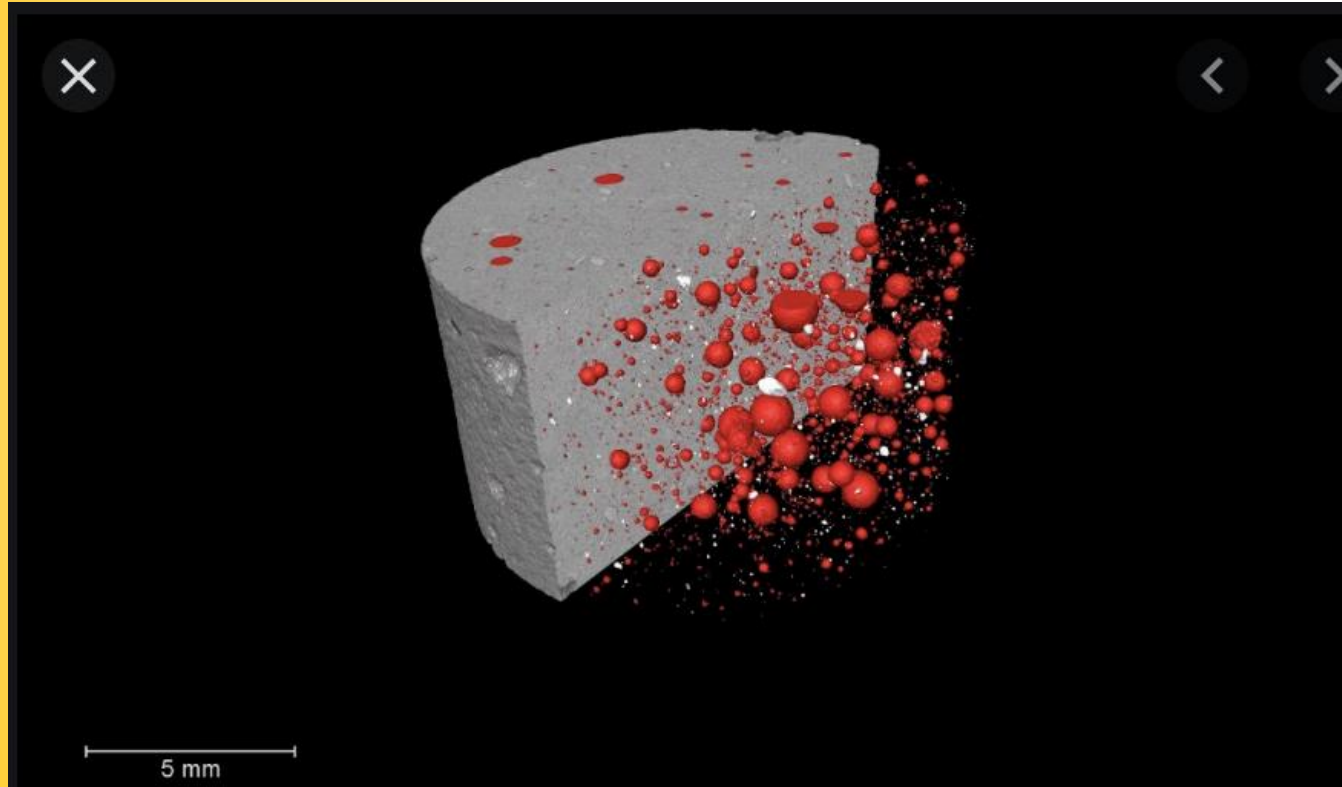
A NEW SENSOR: X-RAY COMPUTED TOMOGRAPHY



<https://werthinc.com/a-new-sensor-x-ray-computed-tomography/>



X-Ray Tomography



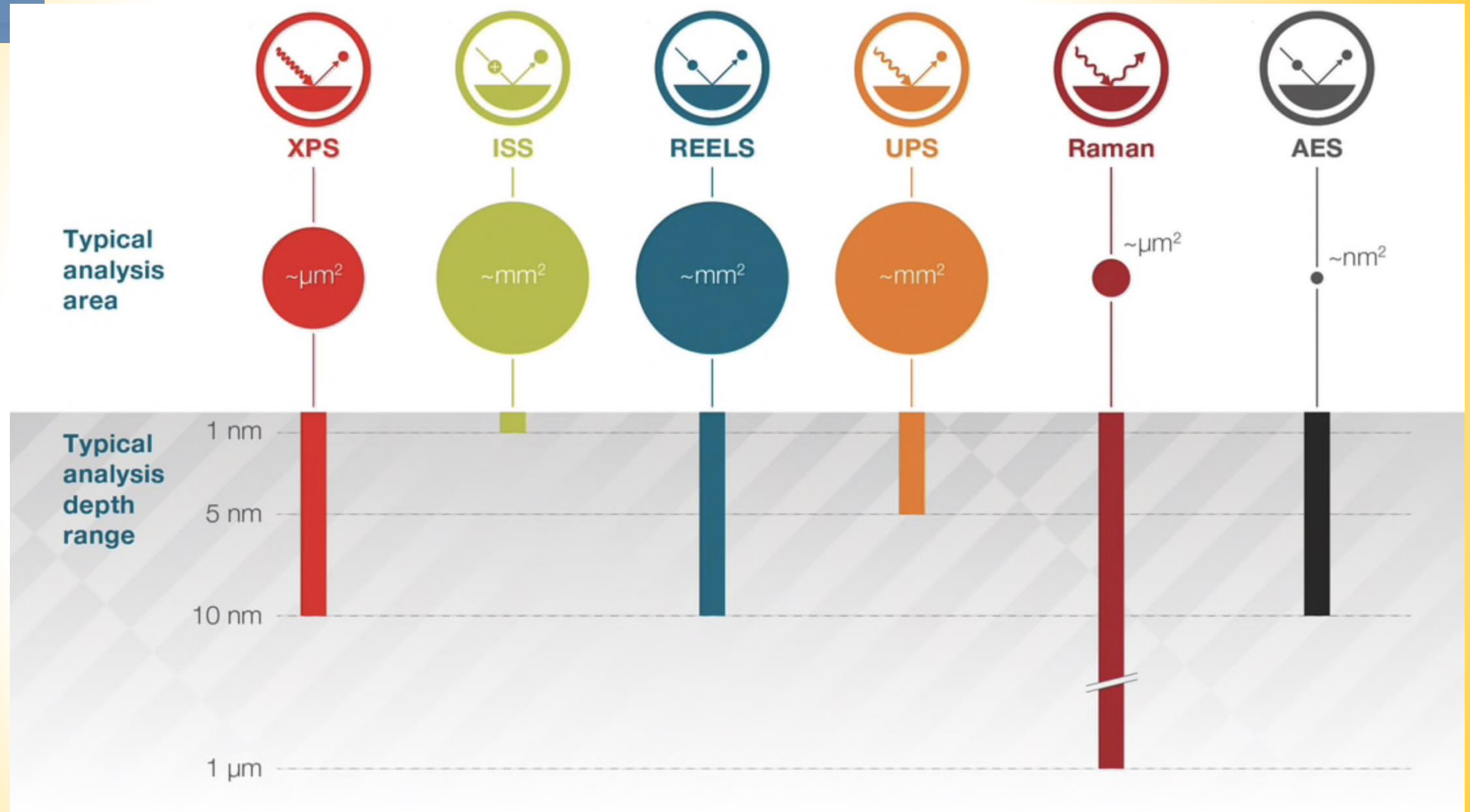


https://www.thermofisher.com/br/en/home/materials-science/xps-technology/multi-technique-workflow.html?cid=2020-ms-xps-multitechnique&utm_source=google&utm_medium=cpc&utm_campaign=2020-ms-xps-multitechnique&gclid=EAlaQobChMI6K333aT_6wIVigaRCh05PA7NEAAYASAAEglcmPD_BwE



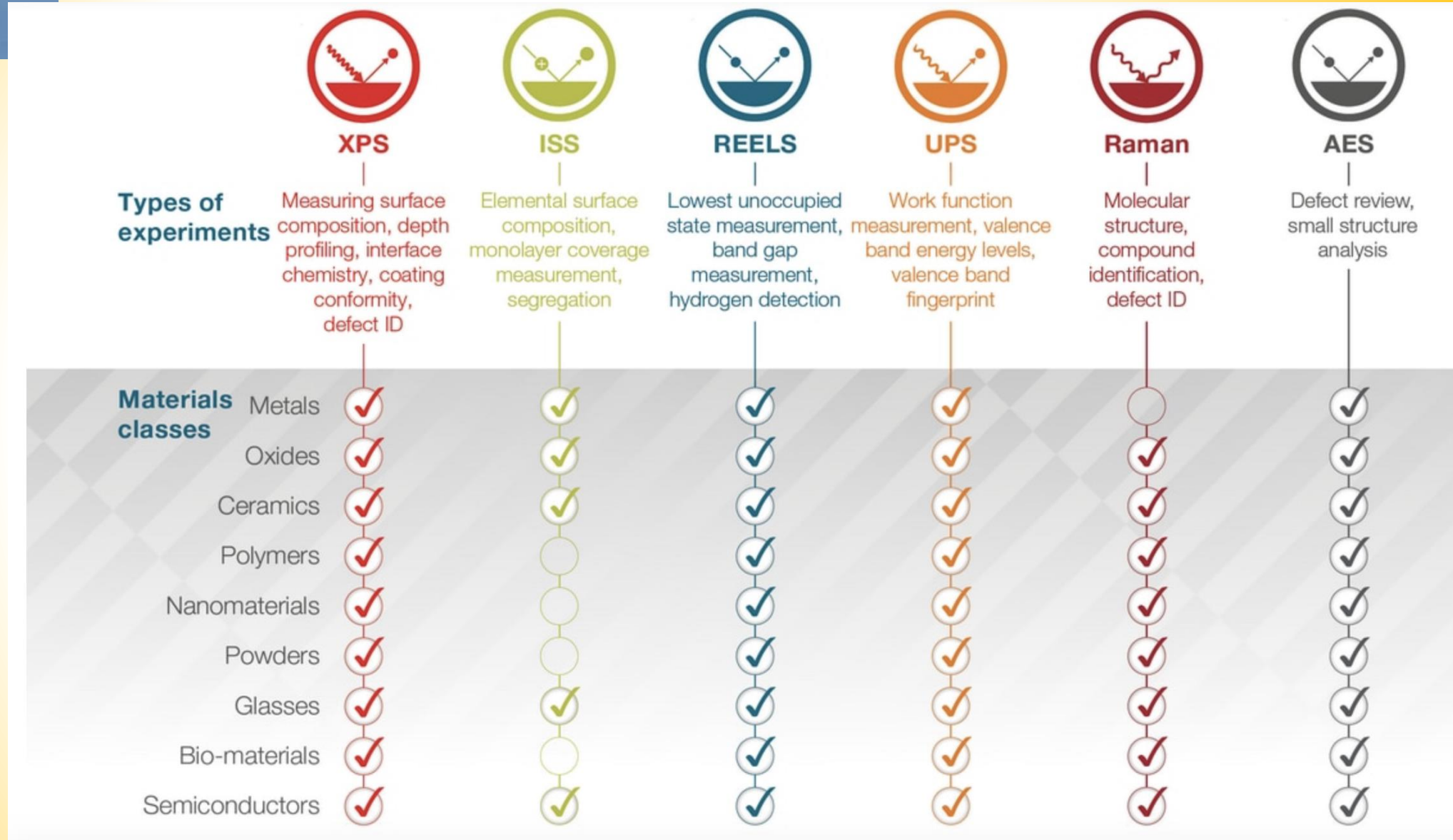


https://www.thermofisher.com/br/en/home/materials-science/xps-technology/multi-technique-workflow.html?cid=2020-ms-xps-multitechnique&utm_source=google&utm_medium=cpc&utm_campaign=2020-ms-xps-multitechnique&gclid=EAlaQobChMI6K333aT_6wIVigaRCh05PA7NEAAYASAAEglcmPD_BwE





https://www.thermofisher.com/br/en/home/materials-science/xps-technology/multi-technique-workflow.html?cid=2020-ms-xps-multitechnique&utm_source=google&utm_medium=cpc&utm_campaign=2020-ms-xps-multitechnique&gclid=EAlaQobChMI6K333aT_6wIVigaRCh05PA7NEAAYASAAEglcmPD_BwE





Hardness

1.2.8 Hardness Measurements

Meyer
Projected area $H = \frac{P}{A}$

Universal (Martens)
Actual area $HM = \frac{F}{4h^2 \sin \theta / \cos^2 \theta} = \frac{F}{26.43 h^2}$

Vickers indenter

$HM = \frac{P}{3\sqrt{3}h^2 \tan \theta / \cos \theta}$

Berkovich indenter

h measured from specimen free surface

Brinell
Actual area $BHN = \frac{2P}{\pi D(D - \sqrt{D^2 - d^2})}$

D = Diameter of indenter
d = diameter of residual impression

Vickers
Actual area $HV = \frac{2P}{d^2} \sin \frac{136^\circ}{2} = 1.8544 \frac{P}{d^2}$

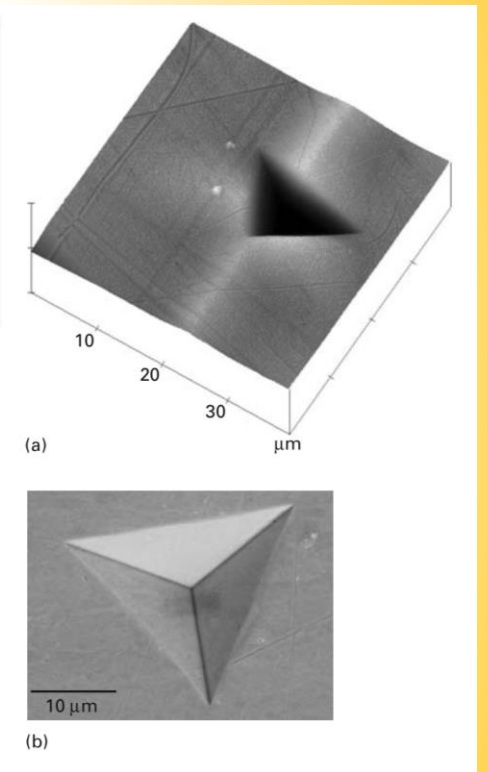
$HV = 0.094495 H$

P = kgf
d = Length of diagonal mm
1 kgf = 9.806 N

Knoop
Projected area $KHN = \frac{2P}{d^2 \left[\cot \frac{172.5}{2} \tan \frac{130}{2} \right]}$

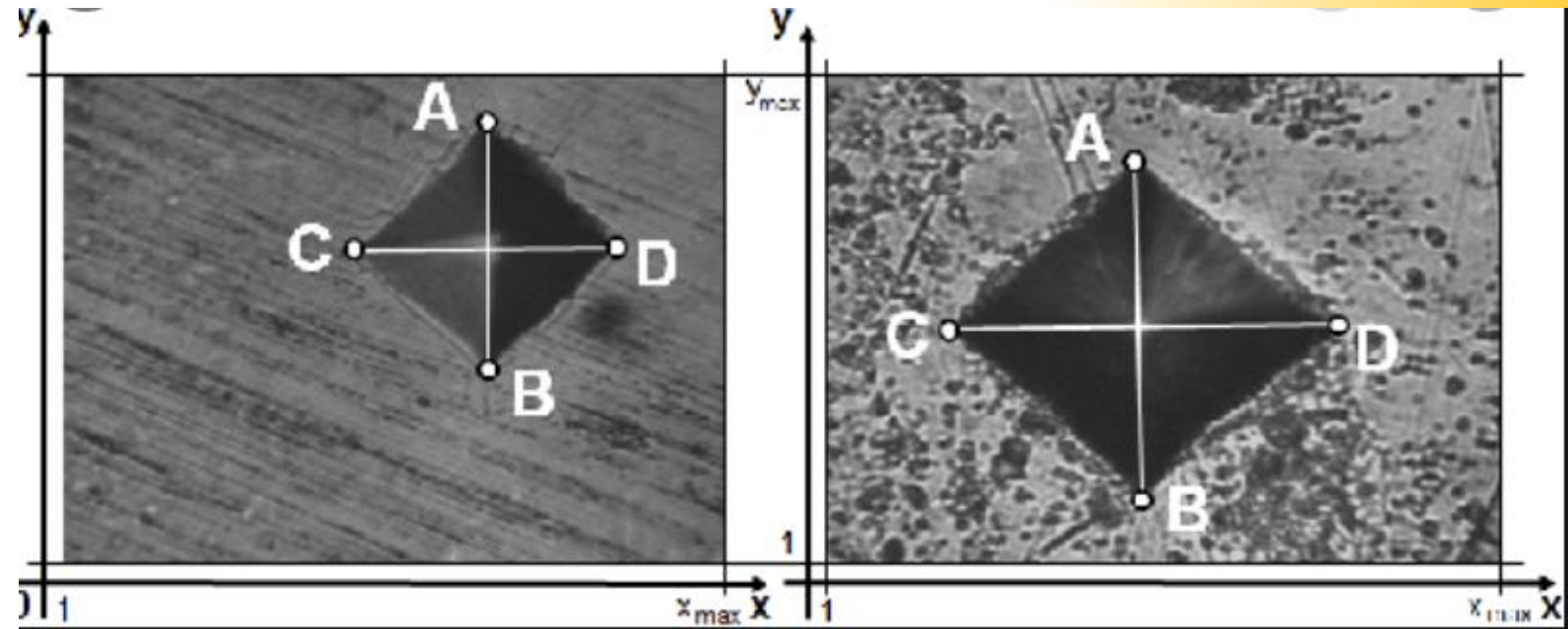
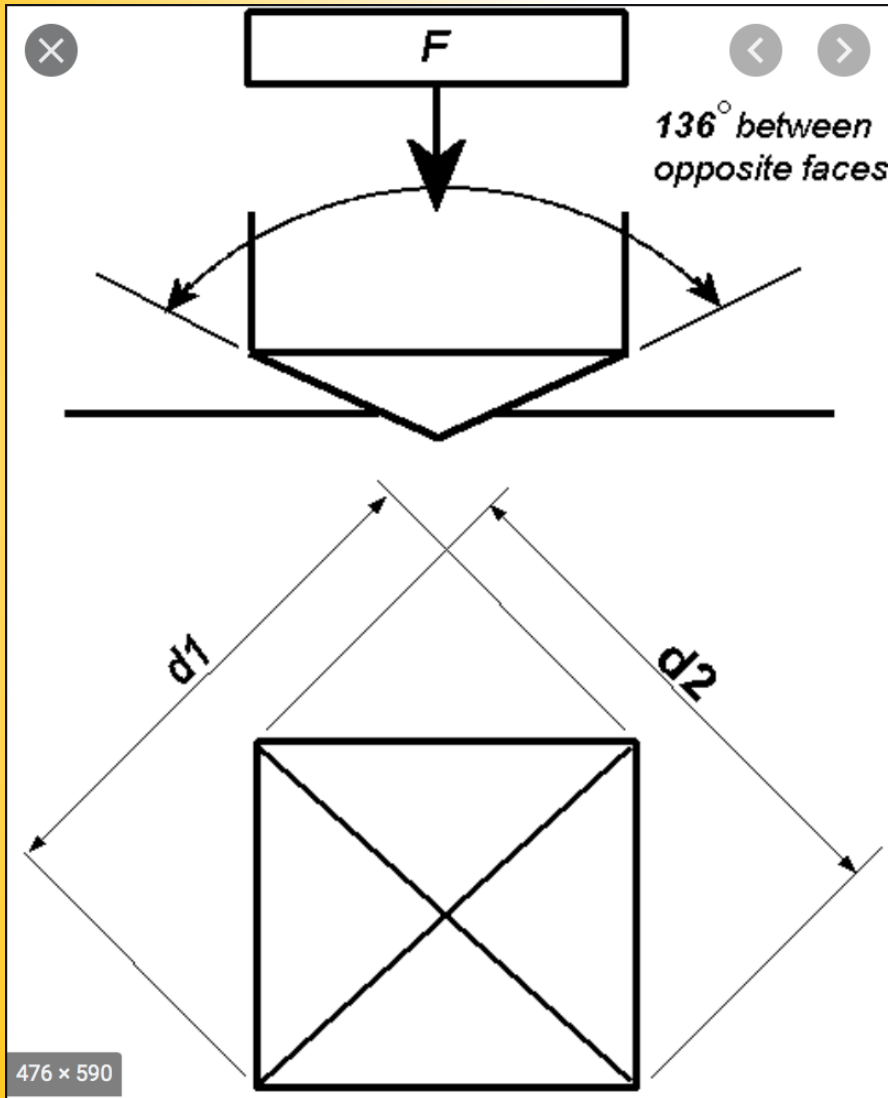
d = Length of long diagonal of residual impression

Fig. 3.42 An impression made by means of Berkovich indenter in a copper sample. (From X. Deng, M. Koopman, N. Chawla, and K. K. Chawla, *Acta Mater.*, 52 (2004) 4291.) (a) An atomic force micrograph, which shows very nicely the topographic features of the indentation on the sample surface. The scale is the same along the three axes. (b) Berkovich indentation as seen in an SEM.



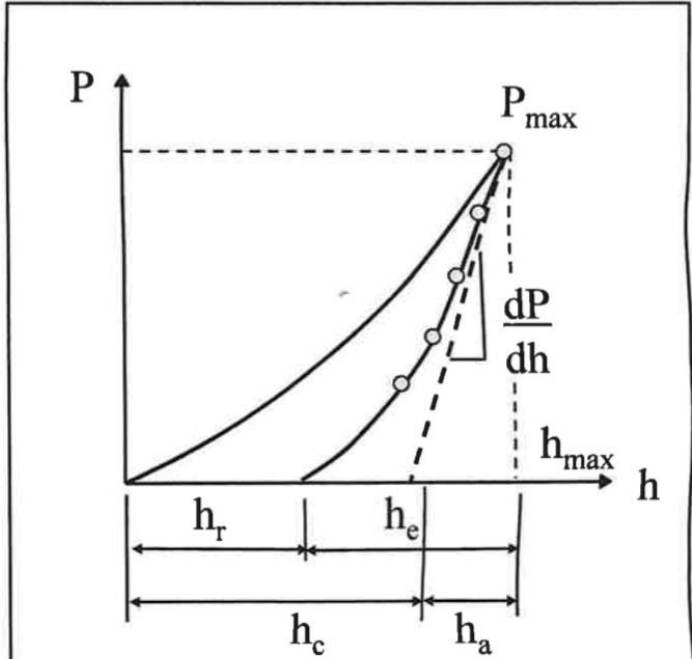


Hardness





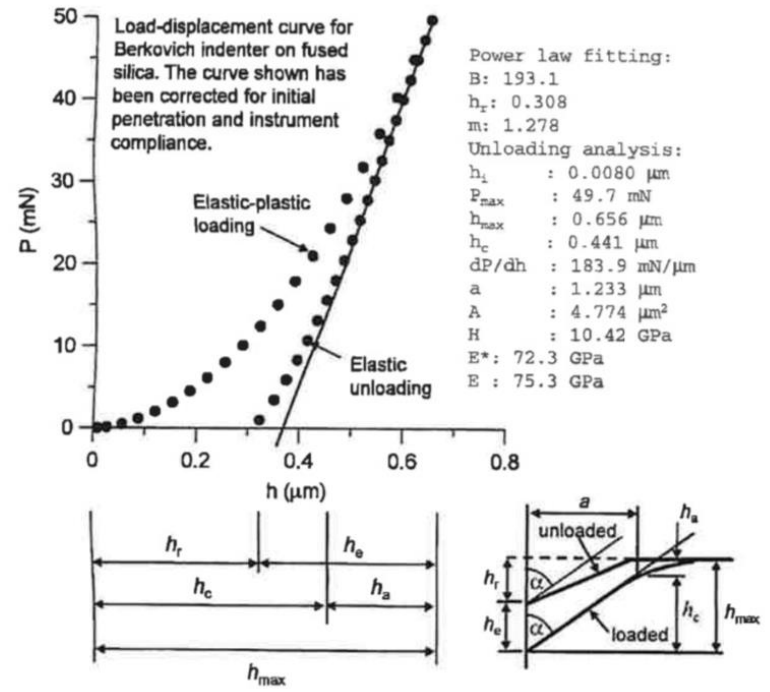
Instrumented Indentation



Analysis of the load-displacement curve allows calculation of elastic modulus and hardness without a direct measurement of the contact area. It is the elastic unloading response that is the basis of the technique.

1.3.1 Load-Displacement Curve

Nanoindentation is conventionally performed using instrumented indentation whereby the load and the indenter displacement are recorded during the indentation process. Both loading and unloading responses are recorded in the form of a load-displacement curve.



Although most nanoindenters are load-controlled machines, it is conventional practice to plot the load on the vertical axis and the displacement on the horizontal axis. The load displacement curve must be corrected for contact depth determination, instrument compliance, and indenter tip shape (area function) before during analysis for the determination of E and H .



Instrumented Indentation

1.3.2 Theoretical Analysis

The load-displacement curve is used to determine the depth of contact by using the elastic unloading data (even if the contact involves plastic deformation). The actual indenter is conveniently modelled as an equivalent conical indenter. The equations of contact are:

$$P = \frac{2}{\pi} E^* h_e^2 \tan \alpha' \quad (1)$$

$$h = \left(\frac{\pi}{2} - \frac{r}{a} \right) a \cot \alpha' \quad r \leq a$$

At $r = 0, h = h_e$:
 $h_e = \frac{\pi}{2} a \cot \alpha'$
 α' is the combined angle of the cone and the sides of the residual impression

At $r = a, h = h_a$:

$$h_a = \left(\frac{\pi}{2} - 1 \right) a \cot \alpha'$$

From which we obtain:

$$h_a = \left(\frac{\pi - 2}{\pi} \right) h_e \text{ and } h_i = h_c + h_a$$

Thus:

$$h_i = h_c + \frac{\pi - 2}{\pi} h_e$$

From Eqn. 1:

$$\frac{dP}{dh} = 2E^* \frac{2}{\pi} h_e \tan \alpha'$$

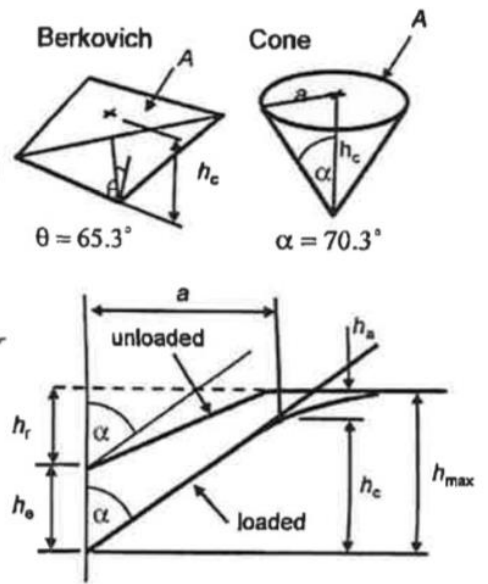
$$P = \frac{1}{2} \frac{dP}{dh} h_e$$

$$h_e = P \frac{2}{dP/dh}$$

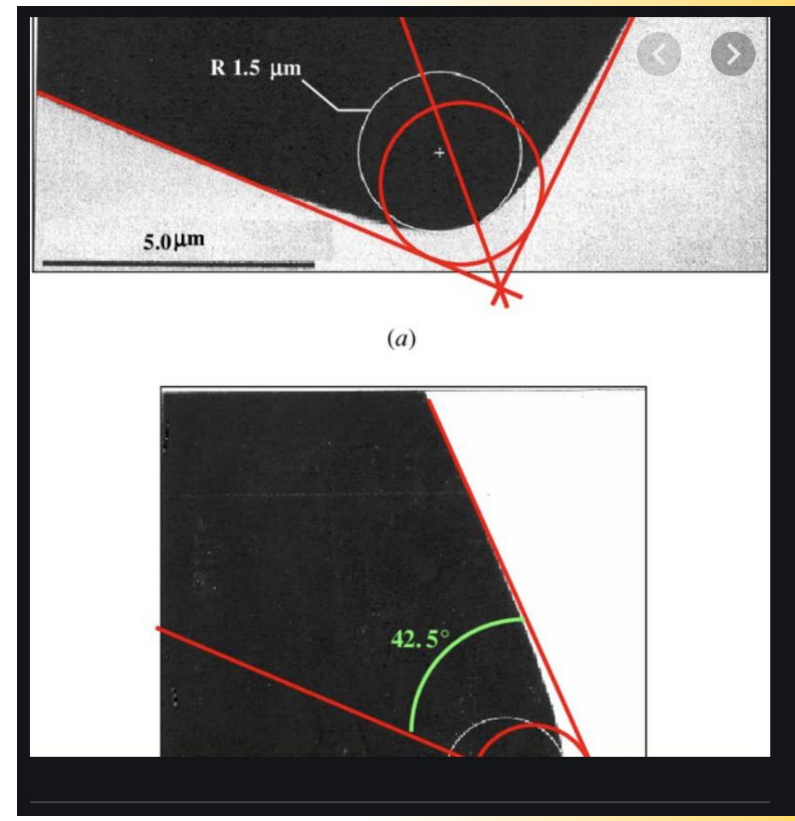
Thus:

$$h_{\max} = h_c + \left[\frac{2(\pi - 2)}{\pi} \right] \frac{P}{dP/dh}$$

h_{\max}, P_{\max} and dP/dh are all obtained from measurements and so h_c can be determined.



Calculation of H	Calculation of E*
$A = 3\sqrt{3} h_c^2 \tan^2 \theta$	$P = \frac{2}{\pi} E^* h_e^2 \tan \alpha$
$= 24.5 h_c^2$	$\frac{dP}{dh} = 2 \frac{2}{\pi} E^* h_e \tan \alpha$
	$h_e = \frac{\pi}{2} a \cot \alpha$
	$\frac{dP}{dh} = 2E^* \frac{2}{\pi} \frac{\pi}{2} a$
	$= 2E^* a$
$H = \frac{P}{A}$	$E^* = \frac{dP}{dh} \frac{1}{2} \frac{\sqrt{\pi}}{\sqrt{A}}$

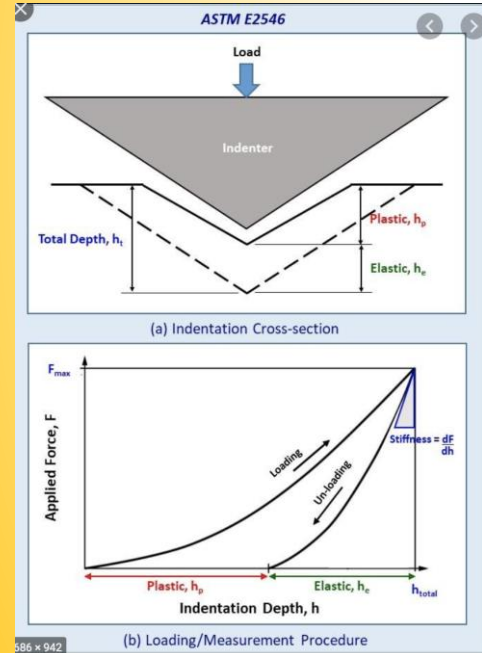


1.3.3 Oliver and Pharr Method

Two of the most important physical properties of materials are elastic modulus and hardness. In nanoindentation, the depth of penetration of a diamond indenter is measured along with the prescribed load. The resulting load-displacement response typically shows an elastic-plastic loading followed by an elastic unloading. The elastic equations of contact are then used in conjunction with the unloading data to determine the elastic modulus and hardness of the specimen material.



Instrumented Indentation



586 x 942



Residual impression of Berkovich indenter in hardened steel.

The three-sided Berkovich indenter is the most popular choice of geometry for nanoindentation testing. The contact depth (as measured from the total depth of penetration) is given by:

$$h_c = h_{max} - \epsilon \frac{P_{max}}{dP/dh}$$

The factor ϵ depends upon the indenter shape. Once h_c is known, the area of contact A is found from the geometry of the indenter.

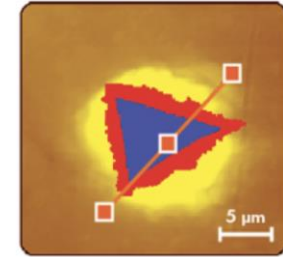
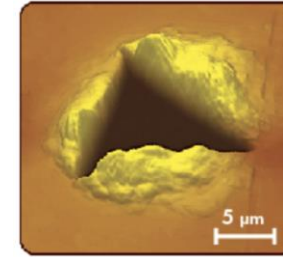
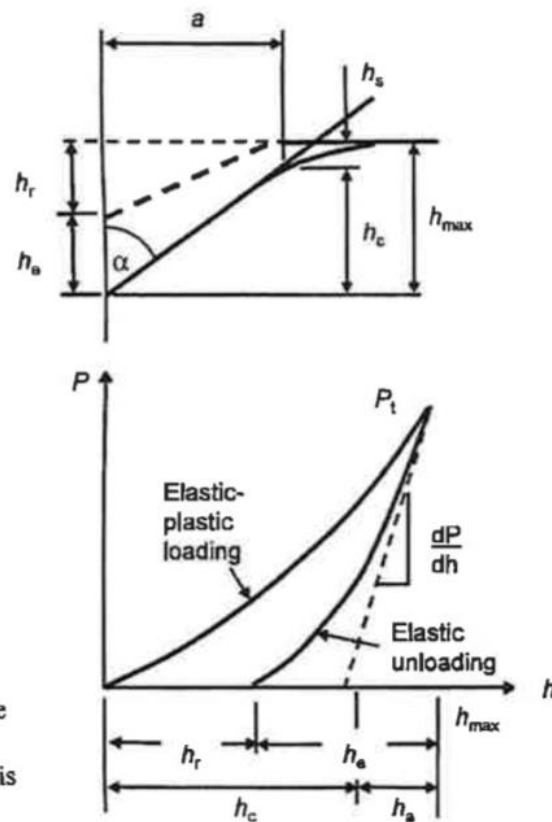
Elastic modulus is given by:

$$E^* = \frac{dP}{dh} \frac{1}{2} \frac{\sqrt{\pi}}{\sqrt{A}}$$

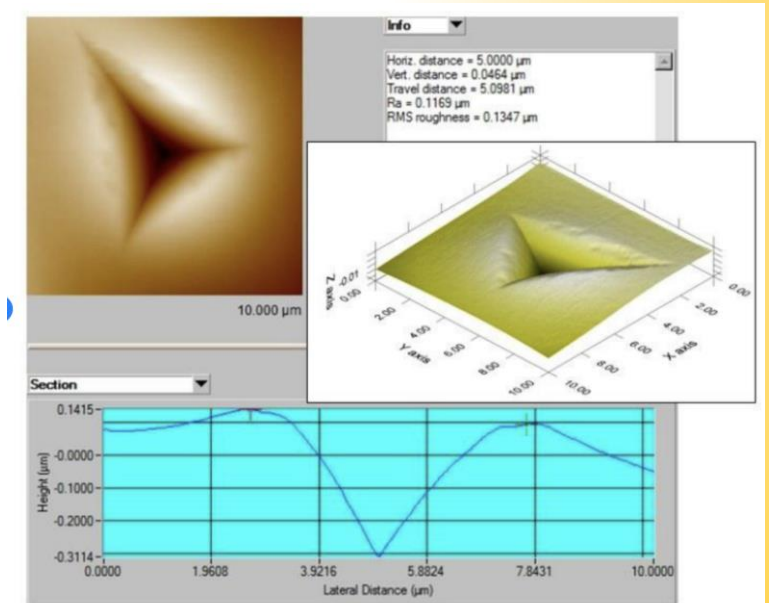
Hardness is calculated from:

$$H = \frac{P}{A}$$

Oliver and Pharr method



<http://nanoscan.info/eng/methods/hardness-measurement-over-the-residual-indent-image>



2D and 3D view (axis dimensions, μm) of the plastic nano-indentation imprint with the corresponding line scan and median roughness for the blend film with 20 wt. % of chitosan.

https://www.researchgate.net/figure/2D-and-3D-view-axis-dimensions-mm-of-the-plastic-nano-indentation-imprint-with-the_fig4_257998720



References

http://www.fhi-berlin.mpg.de/acnew/department/pages/teaching/pages/teaching__wintersemester__2014_2015/elena_willinger__fundamental_of_x-ray_diffraction__141107.pdf